




8-2020

High-Resolution Timeseries Analysis of Dynamic Geochemistry: A 27-Well Survey of Contaminated Groundwater Downstream of the former S-3 Ponds, Oak Ridge, Tennessee

Emma Dixon

The University of Tennessee, Knoxville, edixon7@vols.utk.edu

Follow this and additional works at: https://trace.tennessee.edu/utk_gradthes

 Part of the [Environmental Engineering Commons](#), [Environmental Monitoring Commons](#), [Geochemistry Commons](#), and the [Hydrology Commons](#)

Recommended Citation

Dixon, Emma, "High-Resolution Timeseries Analysis of Dynamic Geochemistry: A 27-Well Survey of Contaminated Groundwater Downstream of the former S-3 Ponds, Oak Ridge, Tennessee. " Master's Thesis, University of Tennessee, 2020.

https://trace.tennessee.edu/utk_gradthes/6251

This Thesis is brought to you for free and open access by the Graduate School at TRACE: Tennessee Research and Creative Exchange. It has been accepted for inclusion in Masters Theses by an authorized administrator of TRACE: Tennessee Research and Creative Exchange. For more information, please contact trace@utk.edu.

To the Graduate Council:

I am submitting herewith a thesis written by Emma Dixon entitled "High-Resolution Timeseries Analysis of Dynamic Geochemistry: A 27-Well Survey of Contaminated Groundwater Downstream of the former S-3 Ponds, Oak Ridge, Tennessee." I have examined the final electronic copy of this thesis for form and content and recommend that it be accepted in partial fulfillment of the requirements for the degree of Master of Science, with a major in Environmental Engineering.

Terry C. Hazen, Major Professor

We have read this thesis and recommend its acceptance:

Larry McKay, Qiang He

Accepted for the Council:

Dixie L. Thompson

Vice Provost and Dean of the Graduate School

(Original signatures are on file with official student records.)

**High-Resolution Timeseries Analysis of Dynamic
Geochemistry: A 27-Well Survey of Contaminated
Groundwater Downstream of the former S-3 Ponds,
Oak Ridge, Tennessee**

A Thesis Presented for the

Master of Science

Degree

The University of Tennessee, Knoxville

Emma R. Dixon

August 2020

Acknowledgements

I would first like to acknowledge and thank my primary advisor and mentor, Dr. Terry C. Hazen. He was gracious enough to hire me as an undergraduate research assistant in 2017, when I was in my senior year studying civil engineering. Through his guidance and the guidance of other interdisciplinary students in his laboratory, I gained an increasing interest in environmental engineering research and was exposed to a multitude of scientific fields like microbiology and geology. I have been presented opportunities through his lab that have helped me gain confidence in my academic and scientific capability. In his lab, I not only worked with interdisciplinary scientists, but I was able to network and work with brilliant scientists from national labs and universities across the nation.

I would also like to acknowledge and thank my committee members, Dr. Qiang He, and Dr. Larry McKay. I first met Dr. He as an undergraduate student in his Environmental Engineering I course in the fall of 2016. His passion, enthusiasm, and immense knowledge for environmental engineering was what first made me interested in the subject, and through his other courses, he helped me establish certainty that I wanted to pursue environmental engineering. I first met Dr. McKay through his academic bond and friendship with Dr. Hazen. I became aware of his vast knowledge and expertise of geology through his experience on the committee of other graduate students. I knew I wanted to have him on my committee as a way to expand my knowledge on hydrogeology. I also took a contaminant hydrogeology course which was an absolute pleasure to attend. I loved the structure, content, and discussion that his class offered and learned so much that I had not had the chance to before.

I would also like to thank all the laboratory collaborators at Oak Ridge National Laboratory. Their training, guidance, and constant support and contributions undoubtedly were a

major part in what made my thesis project successful. This includes field technicians and staffed scientists like Kenneth Lowe and Miguel Rodriguez Jr. for being a constant source of mentorship and support, and I am immensely grateful to have worked with all of them.

I would also like to thank the support and guidance of ENIGMA (Ecosystems and Networks Integrated with Genes and Molecular Assemblies). The exposure to such a wide group of expert scientists around the nation not only helped this project become a success but helped me grow as a confident scientist and engineer.

Funding for this project is acknowledged from ENIGMA (<http://enigma.lbl.gov>) at LBNL supported by Office of Biological and Environmental Research US Dept of Energy Contract No: DE-AC02-05CH11231 and funded in part by Oak Ridge National Laboratory under contract DE-AC05-00OR22725.

Finally, I would like to thank my family, friends, and colleagues for helping foster and support my efforts for completing this degree.

Table of Contents

| | |
|-------------------------------------------------------------------------|-----|
| Abstract | vii |
| 1.0 Introduction..... | 1 |
| 1.1 Assessing and Classifying Redox Conditions..... | 3 |
| 1.2 Water Table Effects on Groundwater Geochemistry | 4 |
| 2.0 Goals, Objective, Hypotheses, Question..... | 6 |
| 2.1 Goals and Objectives..... | 6 |
| 2.2 Hypotheses | 6 |
| 3.0 Methodology..... | 7 |
| 3.1 Study Site | 7 |
| 3.2 Sampling Plan and Methods..... | 11 |
| 3.2.1 Groundwater Sampling and Field Testing for Geochemistry..... | 13 |
| 3.2.2 Laboratory Measurements for Geochemistry | 13 |
| 3.3 Modeling | 16 |
| 3.4 Statistical Analysis | 16 |
| 4.0 Results and Discussion | 17 |
| 4.1 Weather Conditions and Water Table Variations | 17 |
| 4.2 Groundwater Geochemistry Trends | 18 |
| 4.2.1 Dissolved Oxygen..... | 23 |
| 4.2.2 pH | 26 |
| 4.2.3 Oxidation-Reduction Potential | 28 |
| 4.2.4 Conductivity | 28 |
| 4.2.5 Comparison of Geochemical Parameters Trends | 30 |
| 4.3 Correlations and Principle Component Analysis on Geochemistry | 36 |
| 5.0 Conclusions and Future Work..... | 41 |
| 6.0 References..... | 44 |
| Appendix A: Areas Downstream of the former S-3 Ponds..... | 48 |
| Appendix B: Summary Statistics..... | 51 |
| Appendix C: Geochemical Parameters and Water Table Elevations..... | 54 |
| Supplemental..... | 66 |
| VITA..... | 67 |

List of Tables

| | |
|------------------------------------------------------------------------------|----|
| Table 1: Time Series Daily Sample Analyses..... | 12 |
| Table 2: MANOVA Significance Levels in Measured Geochemical Parameters | 35 |
| Table 3: Area 1 Summary Statistics..... | 51 |
| Table 4: Area 2 Summary Statistics..... | 52 |
| Table 5: Area 3 Summary Statistics..... | 53 |

List of Figures

| | |
|------------------------------------------------------------------------------------------------------------------------------------------------------|----|
| Figure 1: Former S-3 Ponds and current area at the Y-12 Security Complex | 9 |
| Figure 2: Monitoring Areas Downstream of the Former S-3 Ponds..... | 10 |
| Figure 3: Well selection and spatial distribution for 27-Well Survey | 14 |
| Figure 4: NOAA average rainfall and rainfall during 2019 at Y-12 Security Complex..... | 19 |
| Figure 5: Daily rainfall (cm) and water elevation (m AMSL) in Area 1 | 20 |
| Figure 6: Daily rainfall (cm) and water elevation (m AMSL) in Area 2..... | 21 |
| Figure 7: Daily rainfall (cm) and water elevation (m AMSL) in Area 3..... | 22 |
| Figure 8: Dissolved Oxygen in mg/L for <i>a</i>) Area 1, <i>b</i>) Area 2, and <i>c</i>) Area 3..... | 24 |
| Figure 9: pH for <i>a</i>) Area 1, <i>b</i>) Area 2, and <i>c</i>) Area 3..... | 27 |
| Figure 10: Oxidation-reduction potential in mV L for <i>a</i>) Area 1, <i>b</i>) Area 2, and <i>c</i>) Area 3 | 29 |
| Figure 11: Conductivity in $\mu\text{S}/\text{cm}$ for <i>a</i>) Area 1, <i>b</i>) Area 2, and <i>c</i>) Area 3..... | 31 |
| Figure 12: Area 1 PCA summary (<i>top</i>), PCA plot sorted by date (<i>left</i>) and well (<i>right</i>) | 37 |
| Figure 13: Area 2 PCA summary (<i>top</i>), PCA plot sorted by date (<i>left</i>) and well (<i>right</i>) | 39 |
| Figure 14: Area 3 PCA summary (<i>top</i>), PCA plot sorted by date (<i>left</i>) and well (<i>right</i>) | 40 |
| Figure 15: Area 1 Wells..... | 48 |
| Figure 16: Area 2 Wells..... | 49 |
| Figure 17: Area 3 Wells..... | 50 |
| Figure 18: Area 1 – Dissolved oxygen in mg/L (<i>points</i>) and water table elevation in m AMSL (<i>lines</i>) | 54 |
| Figure 19: Area 1 – Oxidation-reduction potential in mV (<i>points</i>) and water table elevation in m AMSL (<i>lines</i>) | 55 |
| Figure 20: Area 1 – pH (<i>points</i>) and water table elevation in m AMSL (<i>lines</i>) | 56 |
| Figure 21: Area 1 – Specific Conductivity in $\mu\text{S}/\text{cm}$ (<i>points</i>) and water table elevation in m AMSL (<i>lines</i>) | 57 |
| Figure 22: Area 2 – Dissolved oxygen in mg/L (<i>points</i>) and water table elevation in m AMSL (<i>lines</i>) | 58 |
| Figure 23: Area 2 – Oxidation-reduction potential in mV (<i>points</i>) and water table elevation in m AMSL (<i>lines</i>) | 59 |
| Figure 24: Area 2 – pH (<i>points</i>) and water table elevation in m AMSL (<i>lines</i>) | 60 |
| Figure 25: Area 2 – Specific Conductivity in $\mu\text{S}/\text{cm}$ (<i>points</i>) and water table elevation in m AMSL (<i>lines</i>) | 61 |
| Figure 26: Area 3 – Dissolved oxygen in mg/L (<i>points</i>) and water table elevation in m AMSL (<i>lines</i>) | 62 |
| Figure 27: Area 3 – Oxidation-reduction potential in mV (<i>points</i>) and water table elevation in m AMSL (<i>lines</i>) | 63 |
| Figure 28: Area 3 – pH (<i>points</i>) and water table elevation in m AMSL (<i>lines</i>) | 64 |
| Figure 29: Area 3 – Specific Conductivity in $\mu\text{S}/\text{cm}$ (<i>points</i>) and water table elevation in m AMSL (<i>lines</i>) | 65 |

Abstract

Spatiotemporal variability of geochemistry of contaminated groundwater has large implications on overall water quality and ability to respond to remedial applications. Gaining insight into how geochemical parameters in shallow aquifers respond over time can help establish response trends to changing conditions like water table variations and levels of contamination. In this study, a spatiotemporal survey was performed on 27 wells at depths ranging from 3 to 14 m below surface at the Y-12 Complex in Oak Ridge, Tennessee. This was completed to measure diurnal variations in geochemical conditions from water table fluctuations resulting from seasonal and sudden changes in weather in three areas with historically different contamination levels, originating from a single point source of contamination. Measurements were gathered from 27 previously constructed groundwater wells, four days a week, for the span of 17 weeks (70 days) to build a time series of geochemical parameters. In-field geochemical measurements obtained using *In-Situ Aqua TROLL 600™ Multiparameter Sondes* included dissolved oxygen (DO), pH, conductivity, oxidation-reduction potential (ORP), and salinity. Rain and air temperature were tracked using a *HOBOLink RX3000™ Remote Monitoring Station Data Logger*. Groundwater samples were collected and taken for laboratory analysis and include metals, anions and organic acids, total organic carbon, and stable water isotopes. This thesis only presents data on DO, conductivity, ORP, and pH. Testing for other parameters is still underway. Analysis of DO, conductivity, ORP and pH shows that time and water table variations play critical roles in values of some parameters, but not others. Conductivity and DO values showed large variations with changes in water table but responded in different ways. DO exhibited sustained elevated levels with rainfall, while conductivity rebounded to baseline levels. However, this phenomenon was seen to a much lesser extent in wells with historically high amounts of contamination. PCA

analysis showed that DO, conductivity, ORP, and pH in areas of high contamination were more stable throughout the timeseries even under periods of irregular weather patterns. Conclusions suggest water table fluctuations with time have significant effects in controlling geochemical parameters in groundwater. Therefore, it is necessary to have weather and water levels as parameters when establishing baseline geochemistry for any given area.

This material by ENIGMA- Ecosystems and Networks Integrated with Genes and Molecular Assemblies a Scientific Focus Area Program at Lawrence Berkeley National Laboratory is based upon work supported by the U.S. Department of Energy, Office of Science, Office of Biological & Environmental Research under contract number DE-AC02-05CH11231

1.0 Introduction

Understanding fundamental geochemistry is an essential factor in characterizing the subsurface in any given area. It gives insight into ongoing chemical and biological processes as well as insight on groundwater flow patterns and geologic structure. This can be completed on multiple spatial scales, such as the local or regional scale, with varying degrees of sample density to ensure adequate characterization (1-3). Having a basic understanding of subsurface geochemistry has a variety of applications in society from groundwater monitoring and drinking water designations, to remediation applications. Having knowledge of natural groundwater geochemistry can also aid in the development of targeted perturbation studies (4-9).

This thesis describes a spatiotemporal survey of geochemical parameters conducted on three areas that have a history of nitrate and uranium, mixed waste contamination from the same point source. This was done to characterize the subsurface for future projects: by having a general understanding of subsurface geochemical processes, further experiments can be generated with greater precision at different scales. Measuring elapsed time as a central parameter will expose how quickly the geochemistry is changing and can help design future experiments on the appropriate time scale. For example, if significant changes are seen on a weekly, rather than a daily basis, researchers can design experiments with monitoring at appropriate intervals, thus saving resources while still obtaining suitable data. Additionally, if regions within an area show certain geochemical outliers, these can be targeted in future experimental design, saving further resources and unneeded testing.

In addition, using a timeseries approach to a geochemical survey allows for the understanding of how external factors, such as contamination and weather, influence geochemistry. Gaining insight on geochemical changes over time in response to external factors

allows for the development of predictive geochemistry models. Models can then be employed to forecast various geochemical changes of interest and, again, be used as targets in experimental design. Understanding when, how, and to what extent certain parameters change can also aid in determining contaminant levels, flow, and help establish contaminate plumes (10). This can allow for targeted manipulation of independent parameters to influence groundwater geochemistry and eventually aid in the bioremediation and bioimmobilization of nitrates and heavy metals. It is also recognized that subsurface reduction-oxidation (redox) conditions and water geochemistry can change due to fluctuations in water table, so tracking changes in water table over time can help in establishing these effects on geochemistry (11-13). Additionally, microbial activity from subsurface hydrogeologic interactions such as bioavailable moisture, temperature, redox conditions, and pH play a key role in developing bioreductive conditions, so measuring these interactions during weather changes over time can help predict activity (14).

In this study, the focus is on how water table fluctuations (in response to weather changes over time) affect redox conditions and subsurface geochemistry in the presence of uranium and nitrate contamination. To determine subsurface geochemistry, the *In-Situ Aqua TROLL 600™ Multiparameter Sondes* (Fort Collins, CO) were used. As well, the role of extreme weather conditions—i.e. sudden rainfall events versus longer periods of little rain—on soil geochemistry in the presence of contamination was examined. An in-situ weather device, *HOBOLink RX3000™ Remote Monitoring Station Data Logger* (Bourne, MA), at the site was used to measure local weather to relate it to changes in water level and, subsequently, to changes in geochemistry. Various geochemical parameters were collected over 27 wells spanning three areas with different proximities from the contaminated source. Samples from each well were also taken for additional analyses, including Inductively Coupled Plasma Mass Spectrometry (ICP-

MS), High Pressure Ion Chromatography (HPIC), and Total Organic Carbon (TOC). The analysis was completed over four consecutive days per week for 17 weeks. Here, only the *in situ* field geochemistry measurements are presented.

1.1 Assessing and Classifying Redox Conditions

In groundwater, microorganisms utilize reduction-oxidation (redox) processes to obtain energy. This involves the donating and accepting of electrons with electron acceptors in groundwater, therefore producing an oxidation and reduction product. To do so in the most efficient way, microorganisms favor processes that produce high amounts of energy with the least amount of work. In the hierarchy of redox processes, dissolved oxygen (DO) is the most favorable electron acceptor as it produces the most energy per mole of organic carbon. However, if dissolved oxygen is depleted in the groundwater, other, less efficient, electron acceptors are used to carry out the redox process. The threshold between adequate dissolved oxygen (oxygen reducing conditions) and depleted oxygen (where other available electron acceptors are used) is referred to as oxic ($DO \geq 0.5$ mg/L) and anoxic ($DO < 0.5$ mg/L) conditions, respectively. As oxygen is depleted in groundwater, the next favorable redox-sensitive species is utilized, and the cycle continues. In the hierarchy of redox processes, after aerobic respiration (O_2), the next favorable redox process is through nitrate reduction (NO_3^-), manganese reduction (MnO_2), iron reduction (Fe^{3+}), sulfate reduction (SO_4^{2-}), and methanogenesis (CO_2) (15, 16).

Understanding the dominating redox conditions in groundwater is critical in assessing overall groundwater quality, as redox conditions can give insight to interactions between environmental contaminants. Knowing where certain redox conditions are in groundwater can help reveal the extent of contamination as well as pinpoint contaminated groundwater flow paths (17-19). Redox processes can change the behavior of contaminants, for example allowing toxic

metals to become mobilized or immobilized, such as arsenic and uranium, which can adversely affect groundwater quality (17, 20, 21). Identifying redox conditions and conductivity in groundwater has also been used to map contaminant plumes (10, 17, 22), as it is an indicator of biodegradation of organic matter and heavy metal constituents in groundwater. These processes can be utilized to aid in remediation of contaminated groundwater through natural attenuation by augmenting groundwater either through biological means like bioventing or bioremediation or through chemical means like carbon adsorption (4, 23-25).

Groundwater geochemistry in a single aquifer system can be dynamic with respect to spatial distribution, as subsurface geology impacts groundwater flow and recharge through hydraulic conductivity and natural constituents in the groundwater (i.e. coarse-grained or fine-grained soils) through the water-rock interaction (26-30). Contaminated groundwater from point sources are known to have highly variable geochemistry due to redox zones forming from the contamination source (10, 22, 31, 32).

1.2 Water Table Effects on Groundwater Geochemistry

Because of the potentially rapidly fluctuating water table in clayey soils, the capillary fringe (or variably saturated zone) can host highly variable redox conditions. Therefore, understanding the redox conditions in this zone of variable saturation is of high importance to determine water quality parameters as well as potential natural attenuation. The dynamic relationship between oxygen transfer, redox conditions, and water table fluctuations in this zone can allow for favorable conditions for degradation of groundwater contaminants (29, 33, 34). When sudden local weather conditions (such as rainfall events) occur, water can rapidly enter the groundwater system, and depending on the composition of the soil, extreme water table fluctuations can occur rapidly. Additionally, seasonal water table fluctuations happen and are

slower and more gradual. These slow fluctuations in the water table have been shown to approximately double the amount of oxygen transfer in controlled lab experiments (35). Additionally, water table fluctuations have been shown to create favorable conditions for degradation and enhanced biodegradation activity of groundwater contaminants (36). This is due to air entrapment caused by water table fluctuations supplying oxygen to anoxic water and becoming available to facultative anaerobic microorganisms that have developed a resiliency to live in this subsurface region. Additionally, it has been shown that the frequency of changes in the water table can affect the amount of oxygen transfer (11), and thus redox conditions respond to the oxygen transfer and effect groundwater geochemistry this zone.

Changes in the water table elevation have been shown to affect the biodegradation of contaminants (13, 37-41). When first examining contaminant concentrations due to seasonal weather patterns, concentrations generally trend higher in low rain seasons due to less water in the subsurface and lower in wet seasons due to dilution and mixing with rapidly incoming water (24). These weather patterns are typical in most areas, as in the areas focused in this study. This dilution of contaminants usually goes along with spreading of the contaminant plume. Water table variations also increase vertical mixing and volatilization of groundwater contaminants to increased contact between the groundwater and air in the soil (33, 42, 43). Redox conditions in groundwater contaminant plumes are influenced from the organic matter and other reduced components that are leaked into the system (22). It has been shown that changes in the water table can cause a more consumption of nitrate than a non-fluctuating water table (36). In addition, Sinke et al. showed the effect of water levels on redox conditions and biodegradation of toluene in a soil column, and found that repeated fluctuations in the water table, there were significant differences in redox conditions (44).

2.0 Goals, Objective, Hypotheses, Question

2.1 Goals and Objectives

Detect responses in geochemistry due to water table fluctuations

Monitor high-resolution spatiotemporal changes in geochemical parameters, depth to water table and precipitation over 17-week period (July to December), and statistically analyze results to establish response relationships between geochemical parameters and water table variations. This thesis only deals with measurements of DO, conductivity, ORP, and pH. The influence of water table variations on other geochemical parameters will be addressed in future studies.

Establish geochemical models of areas of interest for Oak Ridge Reservation (ORR)

Establish visual models of geochemistry to aid researchers in conceptualizing the subsurface environment downstream of the former S-3 Ponds. This will allow insight on the relationship seasonal weather and changing environments have on certain groundwater geochemical parameters in the presence of varying amounts of contamination. These models can aid in researchers' efforts to choose specific locations, parameters, and times of interest for future groundwater and sediment sampling.

2.2 Hypotheses

- 1) Seasonal and short-term water table variations are expected to cause statistically significant changes in DO, conductivity, ORP, and pH in shallow wells (3 to 14 m depth) near the former S-3 ponds.
- 2) Measurements from wells that are close to the initial water table are expected to show greater changes in parameters than deeper wells.

- 3) Wells in highly contaminated groundwater zones are expected to respond differently to changes in water table than wells in less contaminated groundwater zones.

3.0 Methodology

3.1 Study Site

The specific areas chosen for this survey were three sites downstream of the former S-3 Ponds at Y12 Security Complex in Oak Ridge, Tennessee (Figure 1). The Y-12 Plant was initially built by the US Army Corps of Engineers in 1943 to separate the ²³⁵U isotope using an electromagnetic separation process as part of the Manhattan Project in World War II (45). After the war, the Plant discontinued this process and developed more in industrial manufacturing, engineering, and security development.

The S-3 Ponds (Figure 1) were built in 1951 to receive wastes from the various Y-12 manufacturing events. They consisted of four, unlined impoundment pits around 122 x 122 meters in area, 5.2 meters deep and with each pond having a capacity of 9.5 million liters. From 1951 to 1984 they received around 10 million liters per year of various types of wastes consisting mainly of toxic, corrosive, and radioactive wastes in the forms of uranium, nitrates and nitric acids, and various volatile organic carbons. Y-12 abandoned the use of these ponds in 1984 and began clean-up procedures and neutralization of the waste. They used *in situ* neutralization and biodenitrification for around 16 months to achieve nitrate levels under 50 ppm. The site was officially closed in February 1988 and was capped with a multi-layered RCRA cap and subsequently covered with asphalt as a parking lot. Extensive characterization of the liquid and sludges in the S-3 Ponds have been conducted and found to be consisting of predominantly highly acidic nitrates with moderately high trace metals (46). Through tracer tests, contamination from the former S-3 Ponds have been shown to seep into local groundwater through contaminant

sorption and matrix diffusion to the east and west of the ponds forming separate migration pathways towards nearby Bear Creek. Nitrate plumes have been seen at depths up to 130 meters and distances up to 300 meters in monitoring multiport wells located beneath the ponds.

Area 1 (Figure 2) is adjacent to the former S-3 Ponds to the south and southeast. The top section of geology consists of around 1.5 meters of saprolite, overlain by clay-rich fill. Underlying geology consists of around 7 meters of intact saprolite and then weathered shale bedrock.

Groundwater flows to the south and southeast towards Bear Creek. Area 2 is located several hundred feet southwest of the ponds. The overall geology consists of around 6 meters of fill and saprolite with 2 meters of intact saprolite underneath and then weathered bedrock. The center of Area 2 had some contaminated residuum excavated and replaced with reworked fill that has higher hydraulic conductivity than the native underlying shale. This was done to test remediation of zero-valent iron permeable reactive barrier next to Bear Creek (47-49). Groundwater flows south and southwest towards Bear Creek. Area 3 is directly adjacent to the former S-3 Ponds to the south and southwest. The section used in this study is located in a 10x10 meter plot in the southeast corner of Area 3. The geology consists of around 1 meter of reworked fill and saprolite on top, followed by around 15 meters of intact saprolite and the weathered bedrock.

Contaminated flow moves through separate pathways from both southeast and southwest of the ponds, and flow through all three areas. The southeast pathway moves through Areas 3 and 2, with Area 3 having historically the highest nitrate and uranium of the three areas, and the southwest pathway moves through Area 1 towards Bear Creek.



Figure 1: Former S-3 Ponds and current area at the Y-12 Security Complex

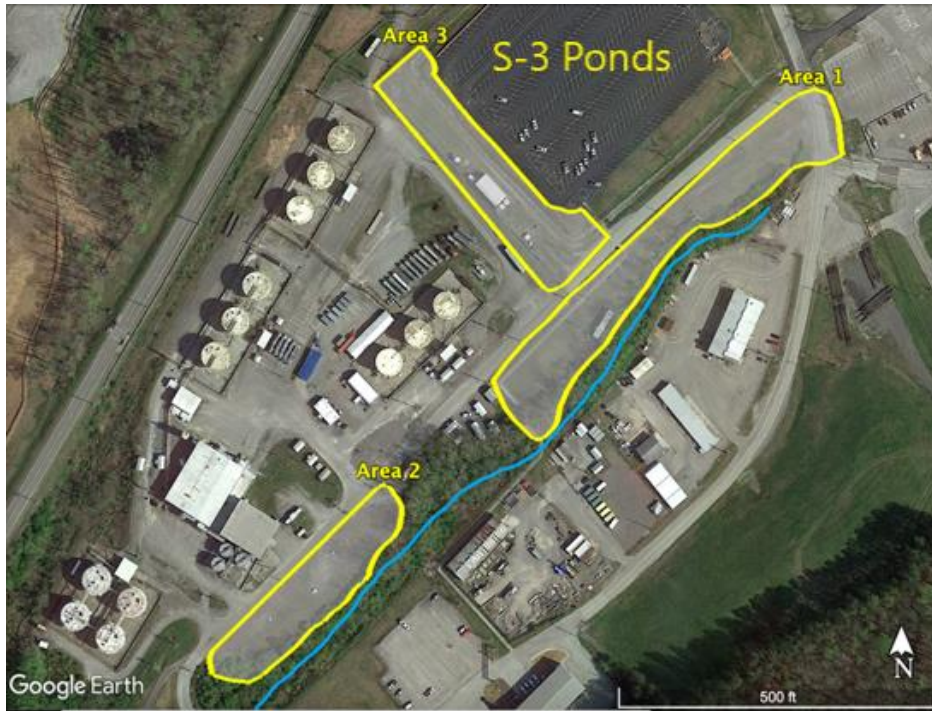


Figure 2: Monitoring Areas Downstream of the Former S-3 Ponds

3.2 Sampling Plan and Methods

A methodology was designed to obtain a spatiotemporal sample set over the course of changing seasons. The analyses taken were chosen based on availability and cost, as well as practicality and ease of daily sampling (Table 1). For example, more costly and time-consuming analyses were taken less often.

The ideal timeline for sampling was four consecutive days per week (Monday-Thursday). Weather played a major role in when sampling occurred. If weather did not permit sampling on a particular day, then any remaining sampling that week were adjusted accordingly. The overall goal was to sample four days within a calendar week. Sampling occurred for a total 17 consecutive weeks with a “pre” sampling date one week before the 17 weeks and a “post” sampling date one week after the 17 weeks. There were three days of the 70 total sampling days that were postponed due to extreme weather preventing field sampling.

Well selection was based on several factors. Since it was required to use previously established wells, the spatial ranges in each area were chosen to maximize area with wells that met all required criteria. First wells that were chosen in each area so all equipment could physically fit inside the well. This translated to wells that had an inner diameter ≥ 2 inches. Secondly, wells were chosen based on spatial location in the areas of interest as well as the physical condition of the well and screen depth. This method allowed for a total of 8 to 10 wells to be chosen at each of the areas of interest, Area 1, Area 2, and Area 3 (Figure 3), for a total of 27 wells. Larger images are in Appendix A.

Table 1: Time Series Daily Sample Analyses

| | Parameter | Samples Taken | Sample Treatment | Analysis Method |
|----------------------------|---------------------------|----------------------|--------------------------------------------------------|------------------------|
| Field Geochemistry | DO, pH, Conductivity, ORP | | | Aqua TROLL 600 |
| | Depth to Water | | | Water Level Meter |
| | Weather Parameters | | | Weather Station |
| Laboratory Geochemistry | Metals | 108/week | 15 mL unfiltered (10 mL injected in Nitric Acid) | ICP-MS |
| | Anions/Organic Acids | 108/week | 2 mL filtered through 0.2 µm syringe filter | HPIC |
| | TOC/TIC/TN/DON | 60/week | 40 mL filtered through 0.2 µm syringe filter | Combustion Analysis |
| | Water Isotopes (2H/18O) | 27/ 4 timepoints | 20 mL, 0.2 µm filtered groundwater | Off-Axis ICOS |

3.2.1 Groundwater Sampling and Field Testing for Geochemistry

To sample each well, first the water level was taken using a *Solinist® Water Level Meter*. Then an *In-Situ Aqua TROLL 600™ Multiparameter Sonde* was placed in each well, and live readings were taken until stabilization was reached (~15 to 20 minutes). Each well was pumped with (indicate type of pump and approximate flow rate) and field parameters were monitored to determine when discharge was geochemically stable. Stabilization was defined as measurements within 5% of the previous measurement for at least five readings. Readings were taken in real-time at around 10 second intervals. Bulk water parameters, including temperature, pH, dissolved oxygen (DO), conductivity, salinity, and oxidation-reduction potential (ORP) were measured. Once stabilization was reached, logging was stopped, and a peristaltic pump was used to purge 1 L of groundwater from the well at around 0.25 L per minute. Once purged, the peristaltic pump was used then to collect groundwater samples using sampling protocols designed for each assay (Table 1). The *HOBOLink RX3000™ Remote Monitoring Station Data Logger* was used in Area 2 to gather weather parameters (notably temperature (°C) and rain (cm)) in 10-minute intervals.

3.2.2 Laboratory Measurements for Geochemistry

Concentrations of metals and trace elements in the groundwater were determined using Inductively Coupled Plasma Mass Spectrometry (ICP-MS) by Dr. Mike Adam's laboratory at the University of Georgia (UGA). For determination of dissolved elements, 15 mL unfiltered groundwater were collected in polyethylene bottles with no headspace. Samples were left overnight at room temperature to allow for adequate and uniform settling of all samples taken that day. To preserve the sample, the next morning 10 mL of the samples were then transferred to 15 mL centrifuge tubes containing 2 mL of nitric acid to maintain a pH of < 2. Samples were stored at 4°C and were shipped to UGA every two weeks.

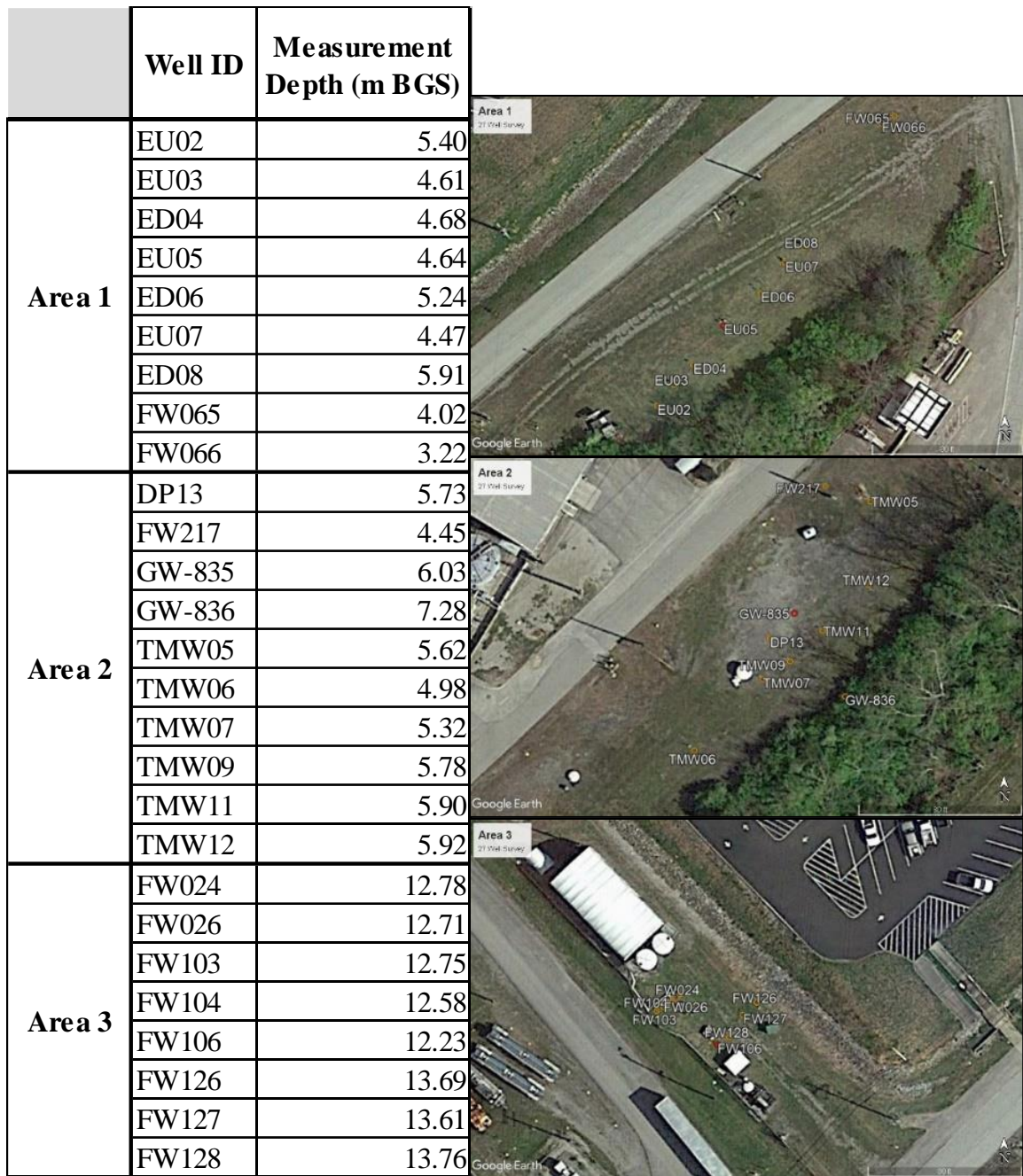


Figure 3: Well selection and spatial distribution for 27-Well Survey

Anions (bromide, chloride, nitrate, phosphate, and sulfate) and organic acids were determined using High Pressure Ion Chromatography (HPIC) by Dr. Dwayne Elias's laboratory at Oak Ridge National Laboratory. IC uses chromatographic separation and conductivity to measure concentration compare with a standardized curve. To determine anions, 2 mL of filtered groundwater was collected in polyethylene vials filled to the top and stored at 4°C until analyzed. For analysis, the samples were loaded and injected into an ion chromatograph. For each sample, the injection loop was flushed to avoid cross contamination. In the chromatograph, the anions are separated and measured. Calibration curves for each analyte were prepared using standard concentrations.

Dissolved organic carbon (DOC) and inorganic carbon (DIC), total nitrogen (TN), and dissolved organic nitrogen (DON) was determined using combustion analysis by Dr. Romy Chakraborty's laboratory at Lawrence Berkeley National Laboratory. Samples were taken for all 27 wells twice a week to reduce costs for testing. Samples were taken on the first and last sampling days every week. In 3 of the 27 wells, EU05, GW-835, and FW106, samples were collected at every timepoint to complete additional daily microbial groundwater analysis. 0.2 µm filtered groundwater samples were collected in injection vials with no headspace. To minimize bacterial decomposition of some components within the groundwater sample, samples were filtered and stored at 4°C.

Stable water isotopes (^2H and ^{18}O) were analyzed by the Stable Isotope Facility at the University of California, Davis using Off-Axis Integrated Cavity Output Spectroscopy (Off-Axis ICOS). Samples were collected at four equally spaced timepoints, 2-week intervals, throughout the timeseries. Specific dates were Wednesdays October 2nd, October 16th, October 30th, and

November 13th. Samples consisted of 20 mL of groundwater filtered through a 0.2 µm syringe filter into sealed vials with no headspace.

3.3 Modeling

The major parameters taken were applied to the *Rockware Rockworks17* program (Golden, CO), with individual visual models being created per parameter, per time point weighted using Inverse Distance (IDW) Anisotropic/Isotropic solid modeling (50). Models were strung together to create a time series model of each parameter for each area. Parameter values for all geological areas in-between wells and in the surrounding areas were interpolated using the inverse-distance kriging interpolation method (51, 52). The kriging algorithm within the morphing tool was used to interpolate parameter values between each timepoint to create a time series film. Models were created to aid in the spatiotemporal visualization of the measured geochemical parameters in each area downstream of the S-3 ponds. From there, certain times and/or areas of interest could be pinpointed and predicted from this investigation for further investigations through sampling groundwater, sediment, or perturbation studies.

3.4 Statistical Analysis

Statistical regression analyses were done on all parameters to test whether any parameters were correlated with one another, and if so, to measure the strength of correlations. This was completed in the coding language R under the *RStudio* framework (53). Samples underwent MANOVA analysis using the *manova* function in the *stats v3.6.2* package. MANOVA, or Multiple Analysis of Variance, is a statistical tool used to test the significance of multivariate data (54, 55). It compares the variance of means of multiple dependent continuous variables and determines their significance following changes of an independent variable while considering interactions between other dependent variables. One of the major assumptions in MANOVA

analysis is normality, therefore all measured parameters were normalized in each well before applying MANOVA analysis. Normalization was achieved visually by graphing histograms with the *qplot* function in the *ggplot2* package with 30 bins, as well as obtaining a skewness of < 1 with the *skewness* function in the *moments* package in R (56, 57).

Principal component analysis (PCA) using the *prcomp* function in the *stats v3.6.2* package that comes with R to determine which geochemical parameter characterized the system over time. PCA is a common tool to establish geochemical control parameters in groundwater. It is multivariate statistical analysis that is a useful tool to interpret large amounts of data **(58-61)**. It reduces variables to a few components that show relationships and strength and dominance between parameters. This is done by scaling measurements with different units, applying eigenanalysis of a correlation matrix, and finding a dimensionally consistent way of expressing relationships. PCA is interpreted through unitless loading and score values that show patterns in complex datasets. PCA was used on the to identify the main hydrogeochemical variables governing groundwater chemistry. PCA using the *prcomp* function in R, and PCA biplots sorted by well and by day for each area was performed using the *factoextra* package in R (62).

4.0 Results and Discussion

4.1 Weather Conditions and Water Table Variations

Over the sampling timeframe, there were notable periods of unusual weather (Figure 4). While temperature remained near average seasonal levels, compared to NOAA average monthly rainfall at Y-12, September and October rainfall varied substantially from normal seasonal conditions. Rainfall in September was 3% of the NOAA average for the area, while there was 46% more rain in October than NOAA averages. These weather conditions have been

experienced before in East Tennessee, but were unusual compared to the normal precipitation patterns (63, 64).

Water levels varied throughout the timeseries by a total of 1.95 m, 1.18 m, and 1.73 m in Areas 1, 2, and 3, respectively. Due to the dry conditions in September and early October, water levels decreased in all areas with the most obvious decreases in Area 1 and Area 3, before an increase in water table from rainfall infiltration in mid-October (Figures 5-7). Wells across Area 1 showed corresponding changes in water table (with depth to water ranging from 1.56 to 3.51 m BGS). Groundwater elevations across the area showed a distinct gradient in the groundwater table, therefore groundwater flow, towards Bear Creek. Like Area 1, water levels in Area 3 wells moved synchronized changes in water table in response to rainfall, and a clear direction of water flow was observed to the southeast.

Area 2 also showed increases and decreases in water table in response to rainfall, however, not as sharply as Area 1. Depth to water ranged from 3.35 to 4.63 m BGS with only GW-836 showing steady rates of water table decline over time. Other wells displayed more consistent water table levels overall. Area 2 has a large area of gravel fill from past construction projects in the top 3 m of soil. There was also more overlap of water table levels, having no distinct groundwater flow direction. GW-836 showed the largest variations in water, with the highest water levels initially in Area 2, and then dipped to the lowest water levels during dry conditions. After the October rainfalls, water levels rose again to the highest in the area.

4.2 Groundwater Geochemistry Trends

Summary statistics for all wells in all areas are shown in Appendix B with graphs of all parameters in Figures 8-11. Larger figures graphed against water table elevations are located in

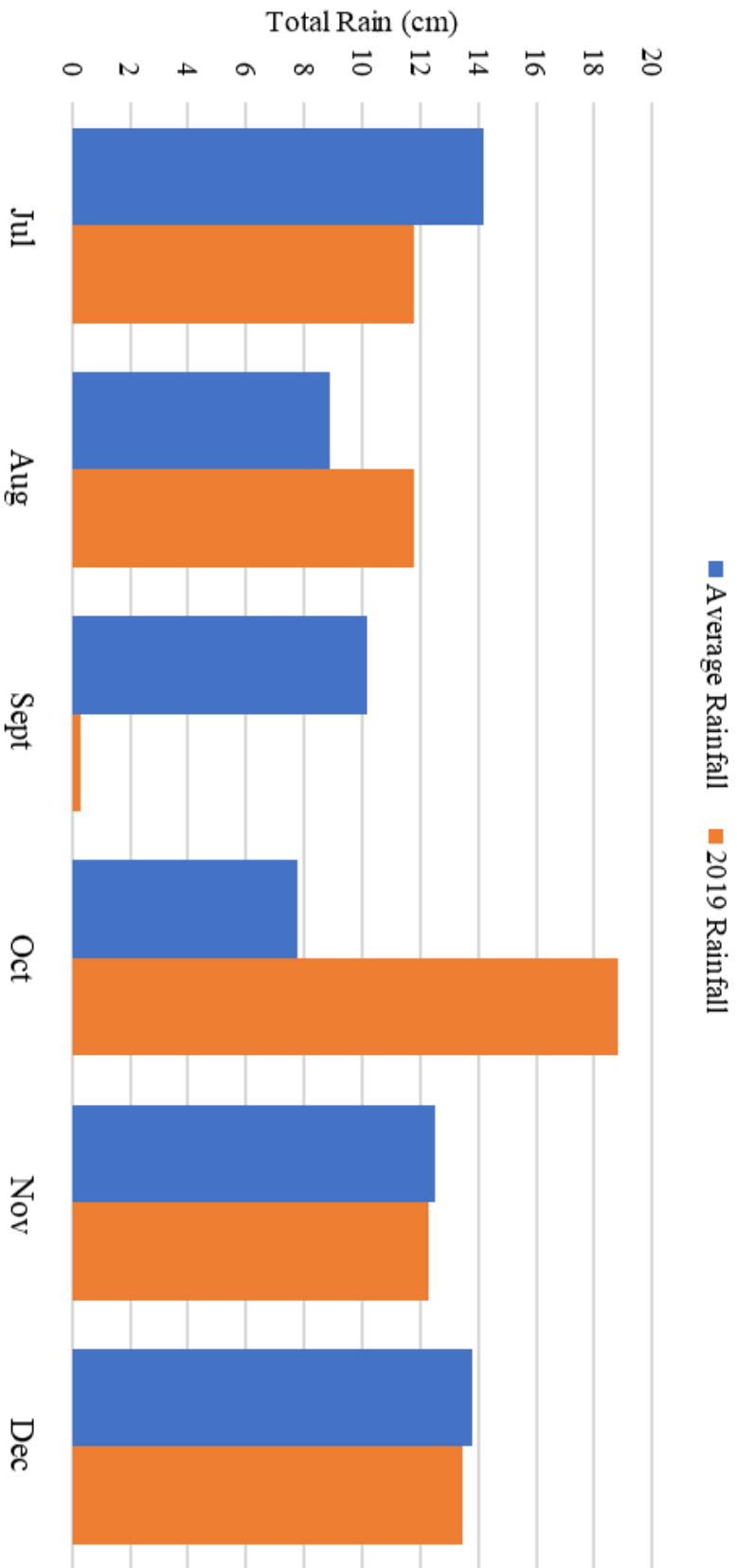


Figure 4: NOAA average rainfall and rainfall during 2019 at Y-12 Security Complex

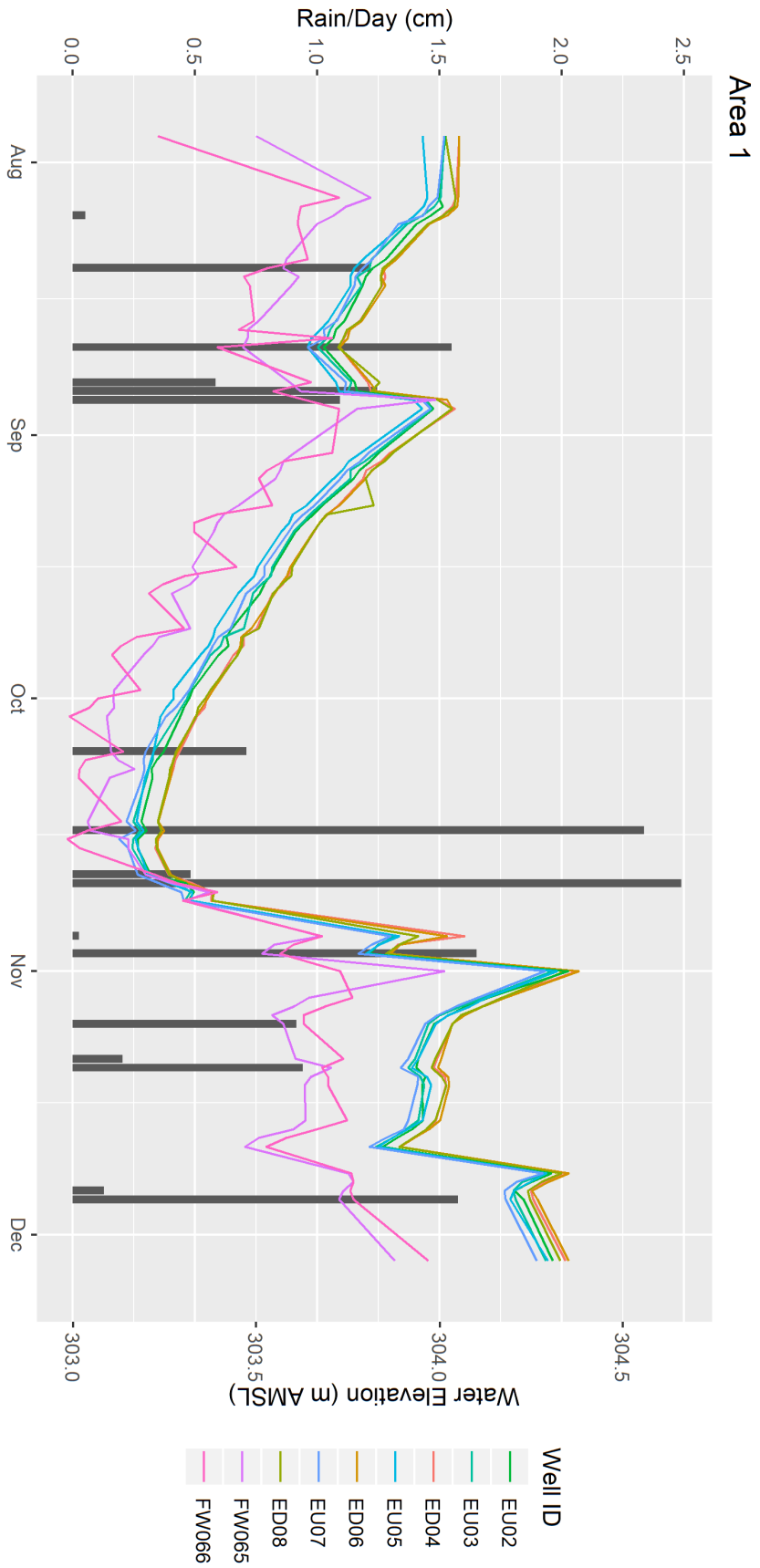


Figure 5: Daily rainfall (cm) and water elevation (m AMSL) in Area 1

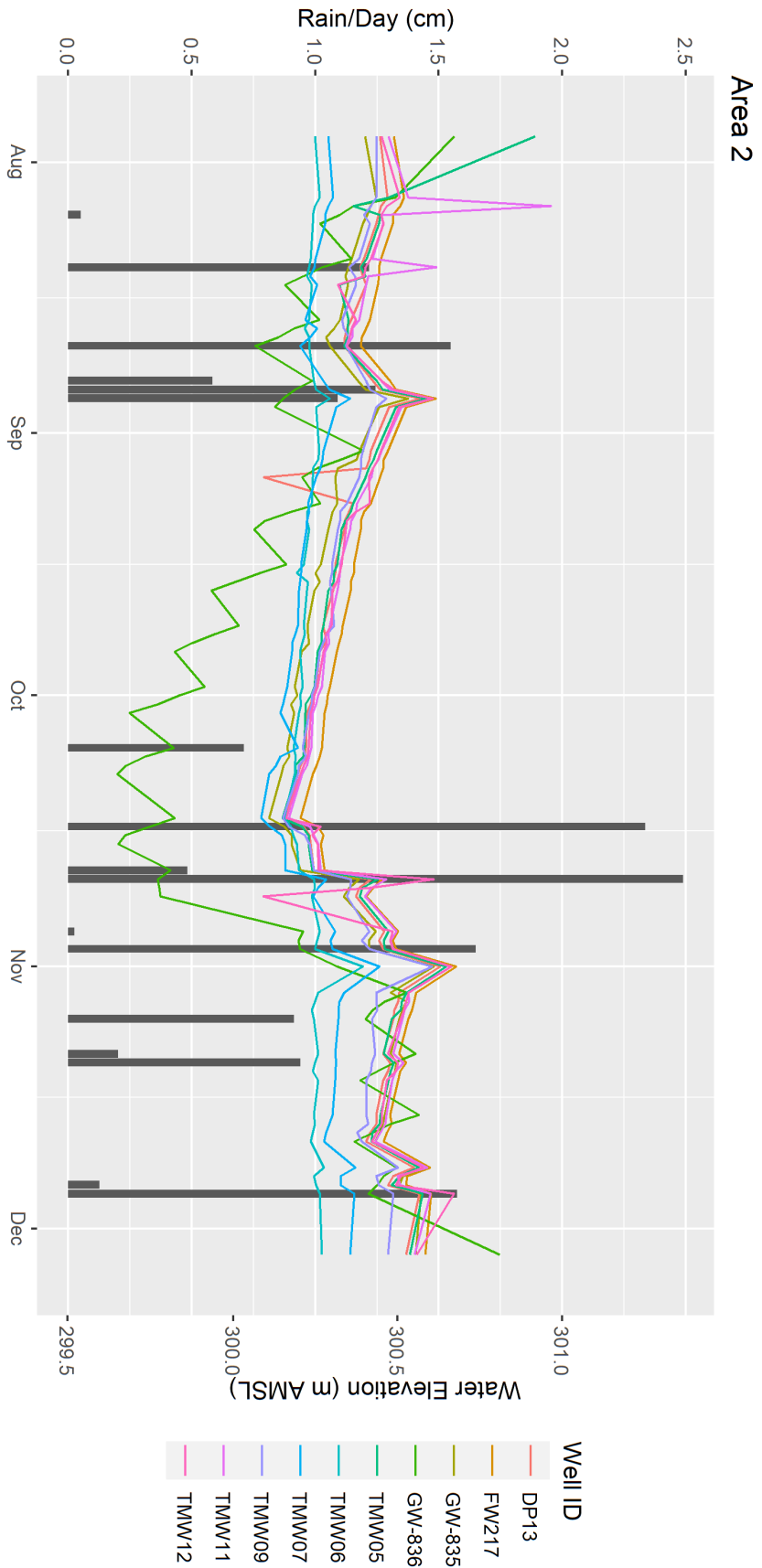


Figure 6: Daily rainfall (cm) and water elevation (m AMSL) in Area 2

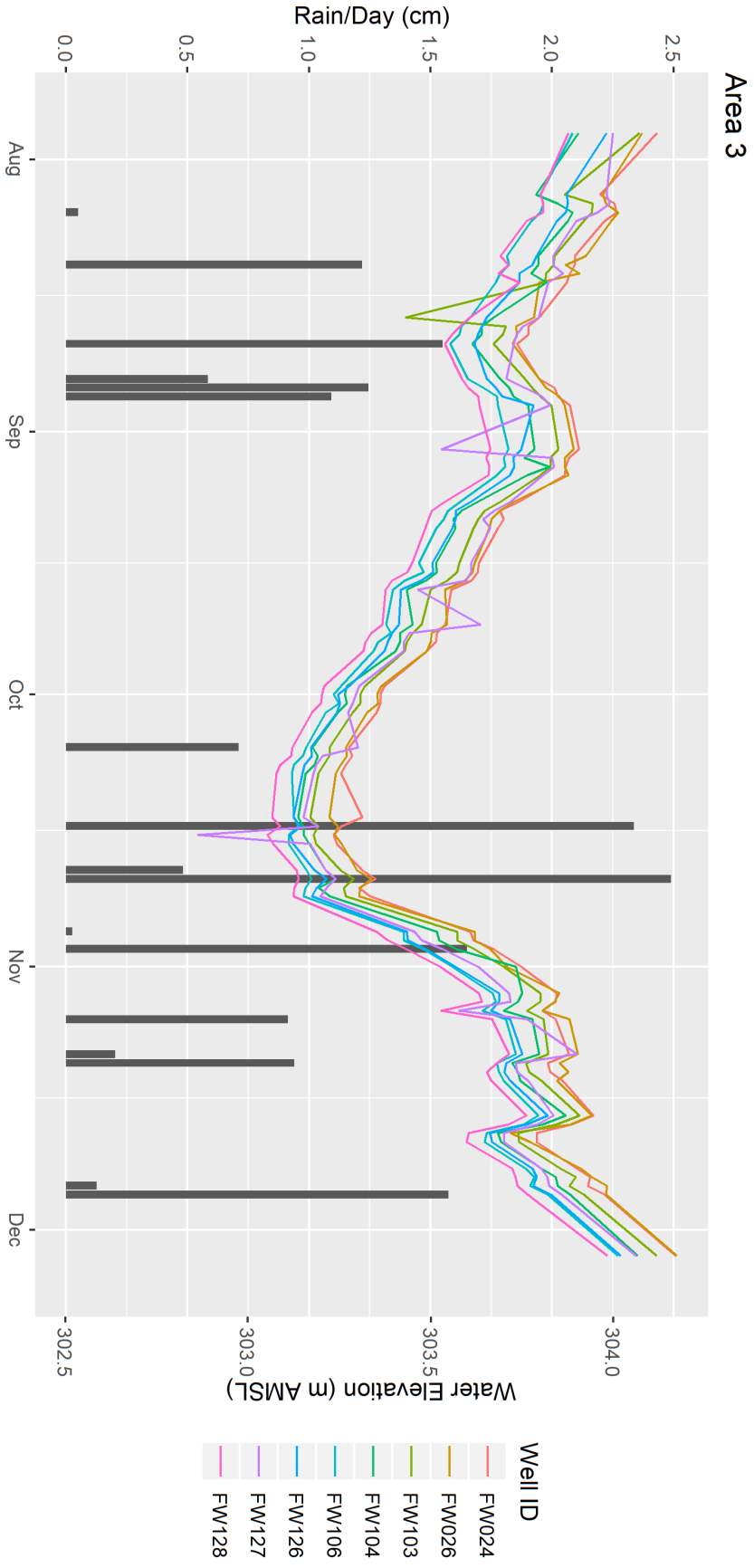


Figure 7: Daily rainfall (cm) and water elevation (m AMSL) in Area 3

Appendix C. The raw data and *Rockworks17* visual models for all areas are in the supplemental file.

4.2.1 Dissolved Oxygen

In Area 1 (Figure 8), FW065 and FW066 had higher conductivity and lower pH throughout the entire campaign. EU07 exhibited significantly higher DO values than all other wells in Area 1 with concentrations ranging from 6.79 to 8.27 mg/L while the next highest DO values, exhibited in EU03 ranged from 0.33 to 5.37 mg/L. EU05 measured lowest ORP levels during specific times (generally moving with a lowering water table) that did not reflect in pH values in the well.

Areas 1 and 2 showed a large range in DO over the timeseries with values ranging from 0 to 8.61 mg/L. Most wells showed slight increases and decreases in DO relative and in response to changes in water table height (i.e. amount of rainfall). This is most observed in Area 1 with EU07, EU05, FW065, and FW066 having sudden, evident increases in DO after the rain inflows in mid to late October. However, DO for all wells in Area 1 exhibited the greatest response not to periods of no rainfall, but to large sudden rain events. Overall, EU07 exhibited much higher DO levels than any other well in Area 1 and showed greatest response to water table variations.

In Area 2, TMW12 measured highest in DO with the largest increases seen with rainfall ranging from 0.06 to 8.61 mg/L, while other wells ranged from 0 to 3.95 mg/L. In contrast to Area 1, more wells showed similar DO values regardless of water table height and rainfall. Only TMW12, TMW11, GW-836, and DP13 showed noticeable increases in DO with rainfall. TMW12, TMW11, and GW-836 are wells nearest to Bear Creek. The consistent DO levels in wells farthest from Bear Creek are likely to be influenced by the steady water table elevations

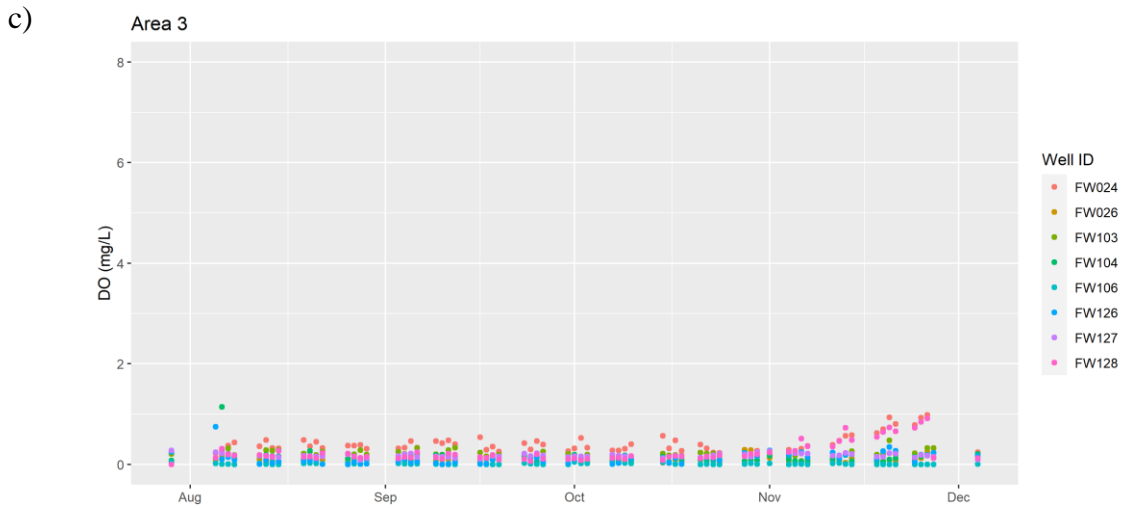
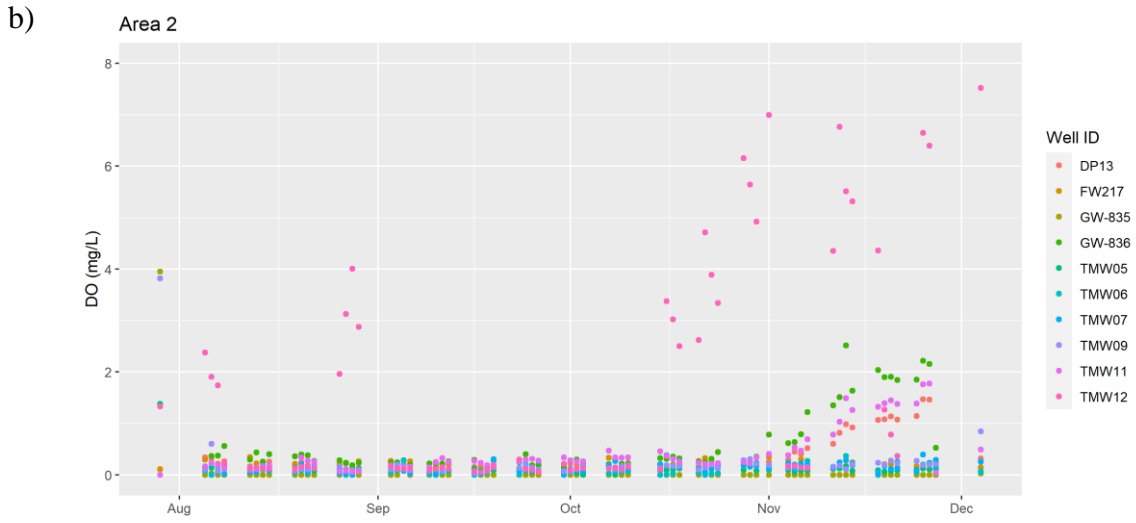
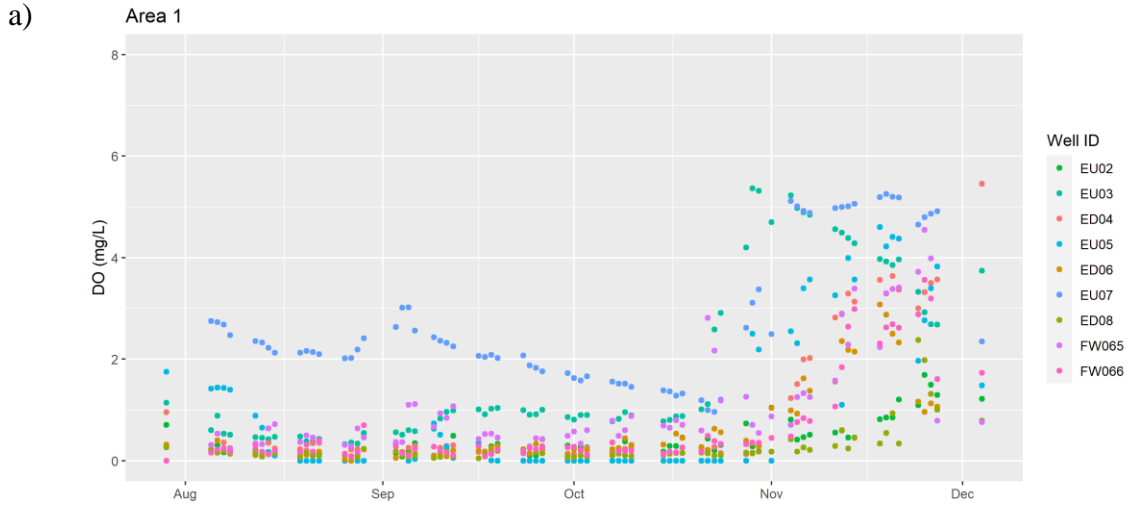


Figure 8: Dissolved Oxygen in mg/L for a) Area 1, b) Area 2, and c) Area 3

and high hydraulic conductivity gravel fill in the center of Area 2. The high conductivity gravel allows rain to easily flow and, unlike the clayey soils near Bear Creek, the DO is not entrapped by any small pore structure. DO in wells closer to Bear Creek exhibit more influence from rainfall and clayey pore structure.

Area 3 experienced a small range of low DO values throughout the timeseries (0 to 1.14 mg/L) with most wells' DO staying relatively constant regardless of rainfall and changes in water table. FW024 measured the highest in DO values throughout, it being the only well in this area to have DO values higher than 0.5 mg/L on multiple days before the significant rainfall in mid-October. Only FW024 and FW128 experienced noticeable response in DO to rainfall in mid to late October.

DO fluctuated between oxic and anoxic conditions in all areas over time. In Area 1, most wells hovered at or just below the threshold for oxic conditions. Only EU07 exhibited oxic conditions for the complete timeseries. EU03 and FW065 displayed oxic levels most of the time. However, after the heavy rainfalls ending the dry period, all wells showed oxic DO conditions and remained oxic for the rest of the timeseries. In Area 2, only TMW12 exhibited oxic DO levels for the entire timeseries. All other wells were continually anoxic until the heavy rainfalls in mid-October. Then only GW-836, TMW11, and DP13 reached oxic conditions, and like Area 1, stayed oxic for the remainder of the timeseries. This pattern suggests varying redox conditions in these areas, fluctuating with oxygen and nitrogen being the dominating electron acceptor.

In Area 3, FW024 (which consistently had the highest DO levels in the area), only reached oxic conditions (0.5 to 0.6 mg/L) at three timepoints before the heavy rainfalls. The three timepoints were after the minor rainfalls during the dry period in September and early October. Other than FW103, which hovered around 0.3 mg/L pre-heavy rainfalls, all other wells

measured DO levels below 0.3 mg/L. Once significant rainfall occurred, FW024 and FW128 reached and maintained oxic conditions.

4.2.2 pH

In Area 1 (Figure 9), FW065 and FW066 measured the lowest pH values over the entire timeseries. There was a distinct gradient in pH values in all other wells in the area with ED08 having the highest pH throughout the timeseries, with pH levels decreasing in each well moving west. Highest pH values were observed in the center of Area 1 (ED08) and decreased to either side (with more significant decreases seen on the east side of Area 1). Similar to results from Mohamed et al. (2003), this could suggest increasing denitrifying conditions as the pH gradient is linear across the wells (65). pH levels in other wells showed more consistent pH.

Similar trends were also observed in Area 2 and Area 3. In Area 2, similar to Area 1, increases in pH were measured when water levels dropped during dry conditions and later decreased with heavy rainfall in mid-October. Most wells consistently hovered just around a pH of 7. Like with DO, there was not an obvious gradient of pH values indicative of groundwater flow or flow paths. The lowest pH values came from GW-835 (in the center of Area 2) and the highest pH values came from TMW09 (also near the center of Area 2).

Area 3 showed lowest pH values overall, but with a larger gradient of pH values throughout this area than in both Areas 1 and 2. This is notable, as Area 3 is the smallest area spatially with the shortest distances between each well. pH was lowest in FW106 and FW126 and highest in FW026 and FW104. Mirroring the other areas, there were increases in pH as water level dropped in the wells. The most noticeable increases in pH values came from wells with the highest initial pH values.

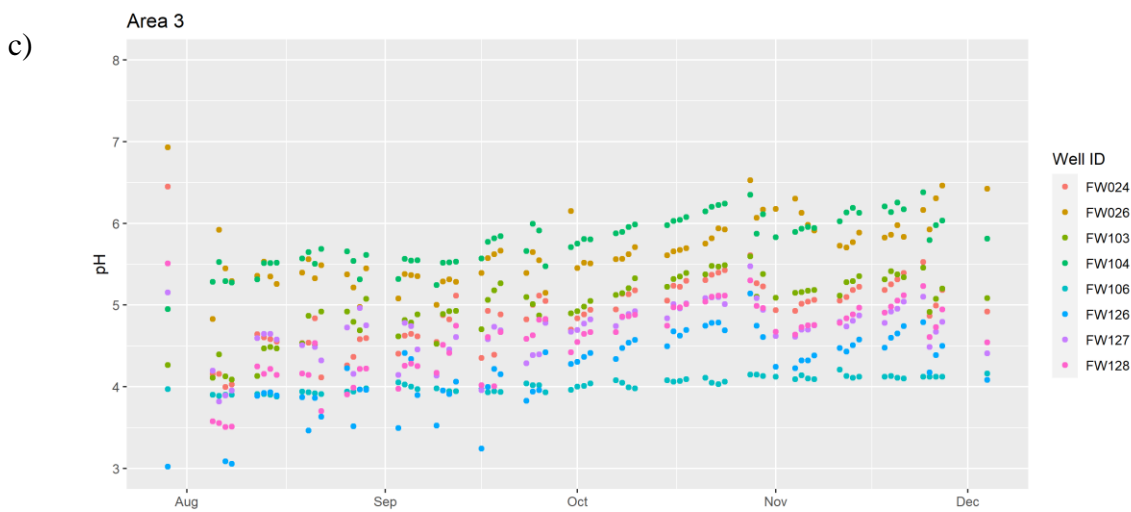
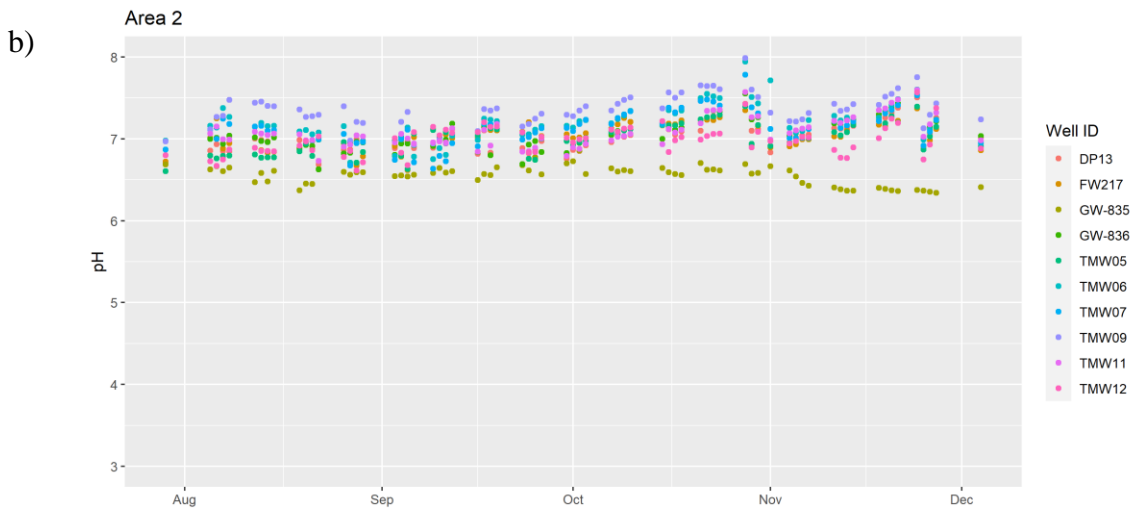
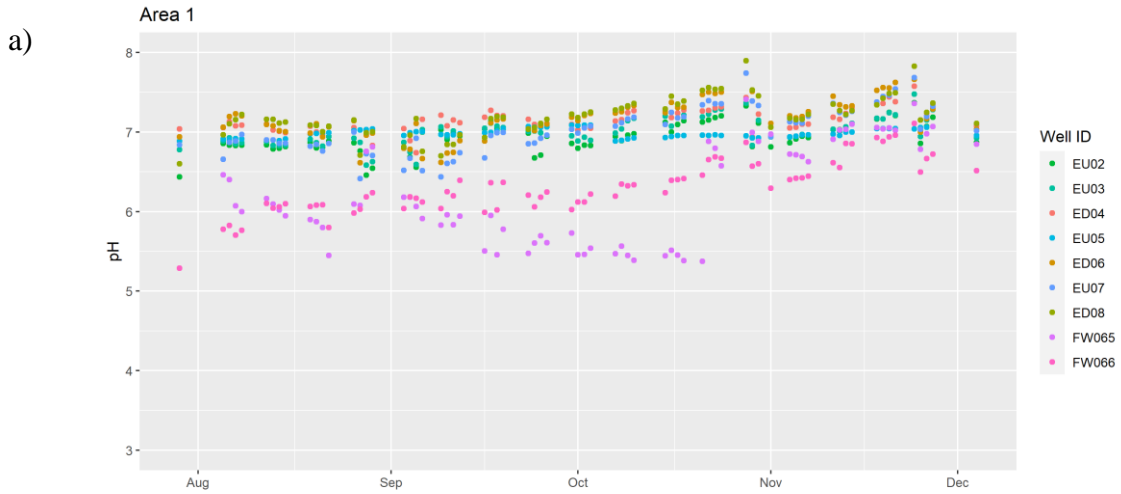


Figure 9: pH for a) Area 1, b) Area 2, and c) Area 3

The higher pH values in Areas 1 and 2 also suggest that carbonate rich soil is likely influencing pH more than the higher nitrate levels. Since the pH of rainwater is around 5, and inflow of rain did not cause significant changes in pH over these two areas, it suggests that the geology of the subsurface is the dominating property controlling pH (66, 67). In Area 3, consistent extremely low pH throughout the timeseries, even with the introduction of higher pH from rainfall, suggests that heavy nitrate contamination is the dominating property controlling pH.

4.2.3 Oxidation-Reduction Potential

ORP values (Figure 10) in all three areas were similar throughout the timeseries with most measurements ranging from 200 to 400 mV. In Area 1, EU05 had the largest fluctuation of ORP levels and was the only well to have ORP levels drop below 0 in mid-October. In Area 2, GW-835 and TMW06 were the only wells to have ORP values drop below 0 mV, although happening at different timepoints throughout the season. While GW-835 is in the center of Area 2, TMW06 is the most southern and most western well in the area and furthest away from the gravel fill. Area 3 demonstrated similar patterns to Areas 1 and 2 but did not have any wells drop in ORP levels below 0 mV. FW126 and FW127 exhibited the highest ORP values for most of the sampling (closest to the former S-3 Ponds).

4.2.4 Conductivity

Conductivity measurements (Figure 11) in Area 1 show FW065 and FW066 having consistently higher conductivity with sharp increases relative to a decreasing water table. Once there were sudden increases in the water table in mid-October, conductivity values in FW065 and FW066 dropped quickly back to

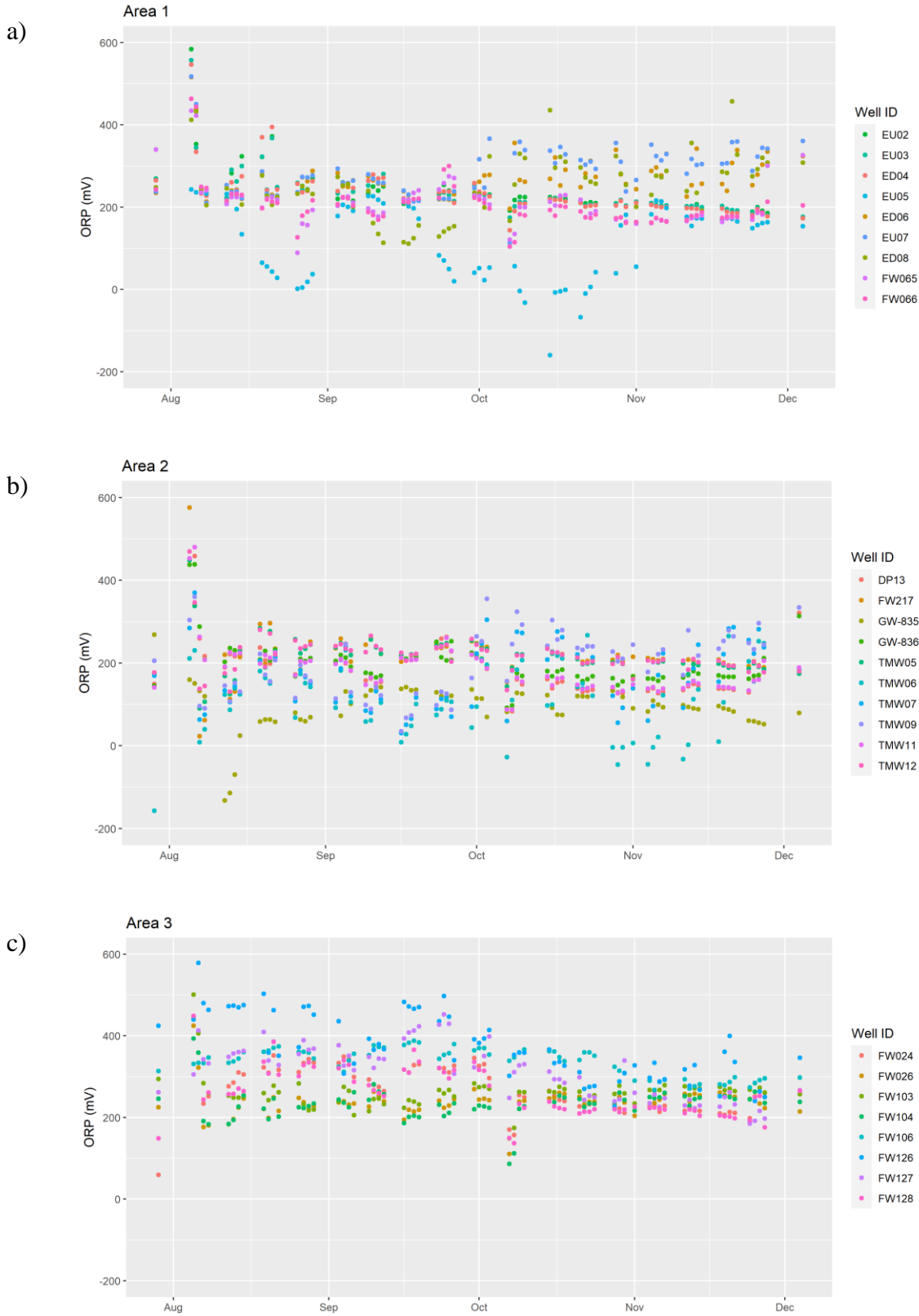


Figure 10: Oxidation-reduction potential in mV L for a) Area 1, b) Area 2, and c) Area 3

previous levels before dry conditions (dropping in FW065 to $< 1500 \mu\text{S}/\text{cm}$ from mid-October to the start of November).

In Area 2, GW-836 and TMW05 had the highest conductivity values throughout the timeseries with the sharpest increases with decrease in water table. Area 3 showed the largest range and significantly higher conductivity values than both Areas 1 and 2 with values ranging from 45.39 to 36,942 $\mu\text{S}/\text{cm}$. FW126 and FW024 showed increases in conductivity during dry conditions from as low as 10,000 to a high of 36,942 $\mu\text{S}/\text{cm}$, then dipping down to $< 20,000 \mu\text{S}/\text{cm}$ in less than a week.

Area 3 has the smallest footprint overall, so the highly variable and extreme conductivity values between wells are noteworthy. Since conductivity is directly related to the number of ions present in groundwater, it is expected that there are significant amounts of total dissolved solids, dissolved salts and other inorganic materials in this area. Additionally, conductivity in all three areas followed the same trends: once rainfall occurred, wells returned to near baseline measurements.

4.2.5 Comparison of Geochemical Parameters Trends

When Area 1 parameters were graphed against changes in depth to water (Appendix C), the only parameters that showed obvious fluctuations in relation to changes in water table are DO and conductivity. When the water table decreased, groundwater DO also decreased in most wells, while conductivity increased. This is mainly due to higher salinity and ions in the groundwater affecting the DO present. However, ORP remained relatively constant in all wells regardless of variations in water table. This suggests resiliency in ORP and high alkalinity against changes in

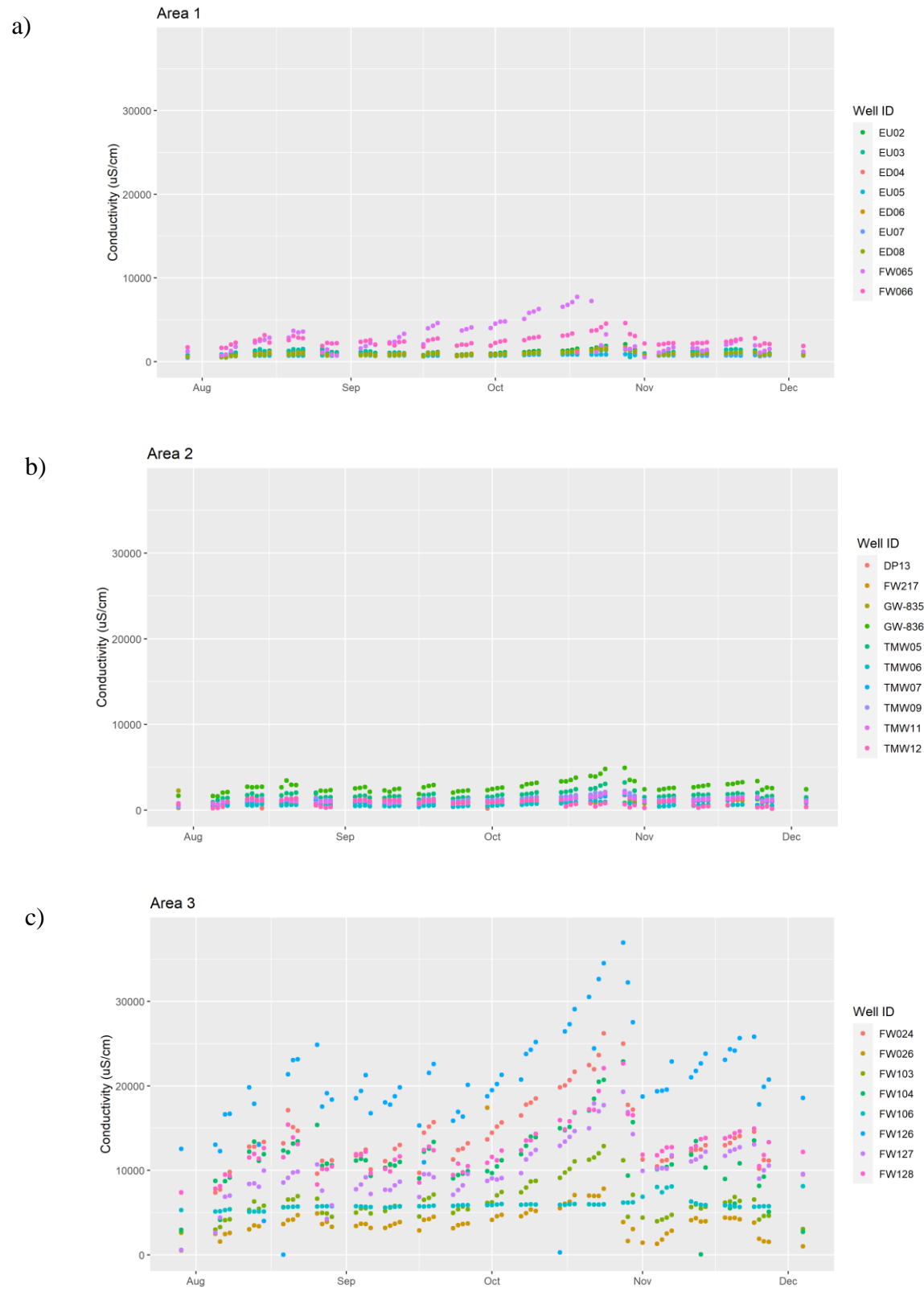


Figure 11: Conductivity in $\mu\text{S}/\text{cm}$ for a) Area 1, b) Area 2, and c) Area 3

sudden water table changes, as well as against changes in DO and conductivity. DO and conductivity are more dependent and vulnerable to water table, since both parameters are shown to be affected by inflows of rain (68). This same trend can be seen in Area 2 with DO and conductivity changing in relation to changes in water table during dry conditions.

However, in both Areas 1 and 2, when DO increased after water table increases in mid-October, it increased to noticeably higher levels than any pre-dry season measurements, and stayed consistently elevated for the rest of the timeseries even as the water table started to gradually decrease from periods of no rainfall. In Area 3, only two wells (FW024 and FW128) exhibited this pattern. FW024 and FW128 are the most central wells in the area and are next to a flat pathway. These wells could either have different source waters or be influenced by the driving pathway that runs along the center of Area 3. This driving pathway could be reinforced with some gravel fill that allows more rainwater to infiltrate these central wells. All other wells had relatively consistent DO levels throughout the timeseries. This suggests that Area 3 groundwater is more heavily influenced by source water from the S-3 Ponds than by the addition or negation of rainfall (even under extreme conditions). DO values are low, and consistently low throughout the timeseries which indicates high contaminant input levels from the S-3 ponds dominating the measured geochemical parameters. The consistently low anoxic conditions seen in Area 3, even with inflow of rain, suggest denitrification is a dominating process in this area.

After each notable rainfall, when water table increased, conductivity dropped to baseline conditions then directly started to steadily increase as the water table decreased. Unlike with DO, conductivity levels in Area 3 showed the same trends as Areas 1 and 2. This reinforces that Area 3 groundwater is more heavily influenced from S-3 Pond source waters than from water table variations due to rainfall. However, with significant differences in conductivity in a much

smaller footprint than Areas 1, it suggests Area 3 groundwater is highly variable. Wells directly next to the S-3 Ponds (FW126 and FW127) exhibited highest ORP and conductivity levels in the area but were average in measurements of DO and pH levels. The wells with highest DO and conductivity values are FW024 and FW128 (wells that are the next closest to the S-3 Ponds). This discrepancy could be attributed to nitrate and metals contamination coming from the ponds increasing conductivity values in wells next to the well but are then diluted when entering the driving pathway in Area 3, and the diluted, oxygen-rich water travels to the next closest wells, FW024 and FW128 (opposite of the driving pathway).

4.3 MANOVA and Principal Component Analysis

When MANOVA was applied to determine significance in geochemical parameters (Table 2), results indicate that Area 2 had the least overall significant change over the timeseries. When considering all wells in each area, 37.5% of Area 2 wells exhibited significant changes in response to water table variations across the four parameters, while 50% and 65.6% of wells exhibited significant changes in Area 1 and 3, respectfully. Per parameter however, results varied. In DO, Area 1 wells showed the greatest change in response to water table variations with 88.9% of wells responding significantly, while only 50% in Area 1 and 62.5% in Area 3. For ORP, 37.5% percent of Area 3 wells responded significantly, while only 11.1% and 10% of wells responded significantly in Areas 1 and 2, respectively. Area 2 wells showed the least amount of significant response to changes in water table at 50%, while 77.8% and 87.5% of wells showed significant responses in Area 1 and 3 wells, respectively. For pH, 22.2%, 40%, and 75% of wells showed significant response to water table variations in Areas 1, 2, and 3, respectively.

A by-well breakdown of significant response to changes in water table reveal that DO and conductivity showed to have highly significant responses in all except FW065 ($p = 0.08339$). Changes in conductivity over the timeseries were shown to be significant in all but EU03 ($p = 0.8859$) and FW066 ($p = 0.1307$). Alternatively, only one well showed significant changes in ORP (EU05) and two wells in pH (FW065 and FW066). This suggests elements influencing DO and conductivity are the most characteristic of Area 1. Additionally, since FW065 and FW066 were the only wells to have shown significant changes in pH over the timeseries, this suggests different source waters may infiltrate these wells with rainfall.

Area 2 showed only half of wells responding significantly in DO and conductivity to changes in the water table. Only one well showed significant change in ORP (TMW05), and three in pH (DP13, FW217, GW-835, and TMW11). Water table variations over the timeseries did not have as great of an effect on wells in this area in comparison to Area 1. Differences in soil type and structure and contaminant levels could affect the DO and conductivity measured in the groundwater in this area.

Overall, Area 3 exhibited the greatest significant change in the geochemical parameters in response to water table variations. Three of the four parameters measured had over half of the wells respond significantly to changes in water table. Five, seven, and six wells responded significantly in DO, conductivity, and pH levels, respectively. Additionally, three wells showed significant ORP responses. The higher significant response in Area 3 wells in ORP and pH suggest that high levels of contaminants like nitrate from the S-3 ponds could be influencing groundwater more than in other areas. Area 3 wells are in the high contaminated groundwater zone directly bordering the former S-3 Ponds. Additionally, since these wells are screened

Table 2: MANOVA Significance Levels in Measured Geochemical Parameters

| Area 1 | DO (mg/L) | ORP (mV) | Conductivity ($\mu\text{S/cm}$) | pH |
|--------------|-----------|----------|--------------------------------------|----------|
| EU02 | 3.88E-05 | 0.7544 | 0.0005499 | 0.3825 |
| EU03 | 0.0001047 | 0.6192 | 0.8055 | 0.1046 |
| ED04 | 2.54E-09 | 0.8244 | 0.000317 | 0.3902 |
| EU05 | 9.83E-13 | 9.56E-08 | 0.03193 | 0.8836 |
| ED06 | 0.0002505 | 0.05601 | 0.0001083 | 0.8443 |
| EU07 | 8.52E-16 | 0.1306 | 0.0001785 | 0.8958 |
| ED08 | 1.12E-07 | 0.2113 | 0.007938 | 0.2814 |
| FW065 | 0.07147 | 0.7146 | 2.20E-16 | 3.23E-10 |
| FW066 | 1.22E-06 | 0.8376 | 0.2713 | 0.02832 |

| Area 2 | DO (mg/L) | ORP (mV) | Conductivity ($\mu\text{S/cm}$) | pH |
|---------------|-----------|----------|--------------------------------------|----------|
| DP13 | 0.004372 | 0.6434 | 0.7837 | 0.06002 |
| FW217 | 0.1244 | 0.6327 | 0.2716 | 0.002009 |
| GW-835 | 0.4392 | 0.221 | 0.0009065 | 7.18E-07 |
| GW-836 | 0.004216 | 0.138 | 0.001362 | 0.04783 |
| TMW05 | 5.78E-05 | 0.06829 | 0.001982 | 0.05034 |
| TMW06 | 0.1878 | 0.3797 | 0.000128 | 0.4148 |
| TMW07 | 0.7655 | 0.8499 | 0.8831 | 0.3995 |
| TMW09 | 0.01276 | 0.913 | 0.05216 | 0.3598 |
| TMW11 | 0.7568 | 0.02039 | 0.8853 | 0.01617 |
| TMW12 | 1.38E-06 | 0.4208 | 1.88E-07 | 0.1344 |

| Area 3 | DO (mg/L) | ORP (mV) | Conductivity ($\mu\text{S/cm}$) | pH |
|--------------|-----------|----------|--------------------------------------|-----------|
| FW024 | 0.5117 | 0.6654 | 7.33E-15 | 0.01628 |
| FW026 | 0.02922 | 0.3589 | 1.93E-10 | 0.4114 |
| FW103 | 0.04295 | 0.04657 | 1.12E-14 | 0.0001793 |
| FW104 | 0.02399 | 0.01391 | 3.00E-06 | 0.003258 |
| FW106 | 0.05634 | 1.61E-06 | 0.8959 | 0.8387 |
| FW126 | 0.0821 | 0.2245 | 0.06885 | 1.25E-05 |
| FW127 | 0.3233 | 0.738 | 1.26E-06 | 0.0001914 |
| FW128 | 0.001765 | 0.1494 | 3.65E-05 | 0.001079 |

*yellow = significant ($p = 0.01 - 0.05$)

*red - highly significant ($p = < 0.01$)

deeper than Area 1 and Area 2 wells, it indicates deeper groundwater depths (13 to 15 m BGS) inducing significant change in ORP and pH when compared to wells screened near the initial water table (4.5 to 9 m BGS), but not in DO and conductivity.

4.3 Correlations and Principle Component Analysis on Geochemistry

When PCA was applied to the entirety of Area 1 (Figure 12), results showed that 91% of the variance in geochemical parameters can be explained in the first three PCA components. pH and conductivity contribute significantly large loadings to the first PCA component and ORP explaining the majority of the second component. The first PCA component expresses the level of proposed contamination in the well, as wells with continuously lower pH values have continuously higher conductivity values. Both nitrate contamination and heavy metals are known to have effects on pH and conductivity in groundwater. Over the timeseries, as changes were experienced in all parameters, changes in pH and conductivity from water table variations had the largest control of measured parameters thus impacting bioavailability of contaminants. This reflects both conductivity and pH both steadily increased with increasing time from last rainfall. The second component expresses the redox conditions of wells (which can also be an indicator of contamination) with ORP having the highest loading. The PCA plot sorted by time (Figure 12) shows different clusters of data values over the timeseries. Early timepoints in August (pre-dry season) show most clustering in the center of the plot and are not being characterized by any single geochemical parameter and has geochemical parameters in a state of balance. There is a small cluster of August timepoints to the bottom left characterized by high conductivity, but from PCA sorted by well, this is due to FW065 and FW066 have uniquely higher conductivity

| Area 1 | PCA1 | PCA2 | PCA3 | PCA4 |
|------------------------------------------|---------|---------|---------|----------|
| DO (mg/L) | 0.1665 | 0.1881 | 0.6411 | 0.0042 |
| ORP (mV) | 0.0647 | 0.7041 | 0.2307 | 0.0004 |
| Conductivity ($\mu\text{S}/\text{cm}$) | 0.7382 | 0.0583 | 0.0381 | 0.1654 |
| pH | 0.7787 | 0.0430 | 0.0017 | 0.1765 |
| Eigenvalue | 1.7482 | 0.9936 | 0.9117 | 0.3466 |
| Variance % | 43.7041 | 24.8388 | 22.7926 | 8.6645 |
| Cumulative Variance % | 43.7041 | 68.5430 | 91.3355 | 100.0000 |

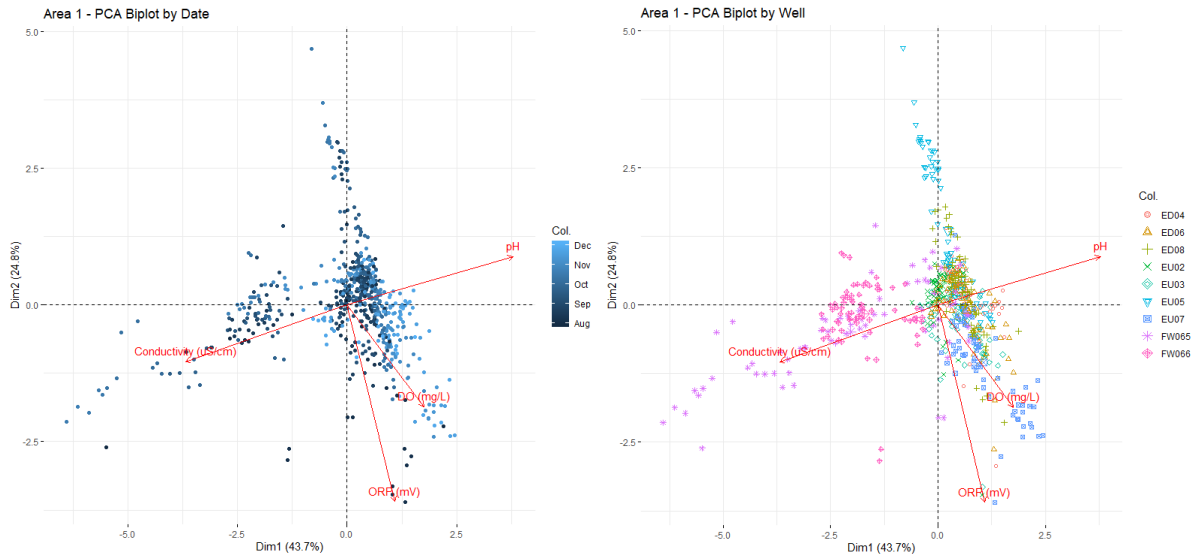


Figure 12: Area 1 PCA summary (top), PCA plot sorted by date (left) and well (right)

values than the rest of the area. During dry weather and low water table levels, measurements clustered towards the upper right and upper center being characterized by changes in pH, with clustering towards DO during the later wet weather and high water table levels. Throughout the timeseries, FW065 and FW066 consistently clustered towards high conductivity values regardless of water table variations. Other well clusters included EU05 clustering to the top and EU07 clustering in the lower-right. The distinct clustering of wells within this one area suggest multiple source water within this area or from possible clay lenses that redistribute groundwater flow in the area.

In Area 2 (Figure 13), 81% of the variance seen can be explained by the first 3 PCA components. ORP, conductivity, and pH all have similar loadings that make up the first PCA component with the second component being predominately DO loaded. This first component expresses contamination, though to a lesser extent than Area 1. There was less distinct clustering of dates throughout the timeseries with only slight pre-dry season clusters forming in the upper-right showing no distinct characterization from a single parameter. When the PCA was sorted by well, GW-836 and TMW12 being notable outliers in the area. This is most likely due to their proximity to Bear Creek, with increasing dissolved oxygen in these wells. Additionally, TMW12 and TMW05 (western most wells in Area 2) clustered towards conductivity. These are the first wells that encounter the source flow from the former S-3 Ponds in the gravel backfilled area and could explain the higher conductivity values.

In Area 3 (Figure 14), 92% of the variance can be explained by the first three PCA components, ORP and conductivity exhibited notably high contributions to the first PCA components with conductivity and DO having similar loadings on the second component. There

| Area 2 | PCA1 | PCA2 | PCA3 | PCA4 |
|------------------------------|----------------|----------------|----------------|-----------------|
| DO (mg/L) | 0.0087 | 0.7747 | 0.0494 | 0.1672 |
| ORP (mV) | 0.3164 | 0.2151 | 0.3511 | 0.1174 |
| Conductivity (μS/cm) | 0.5253 | 0.0902 | 0.0168 | 0.3678 |
| pH | 0.4336 | 0.0035 | 0.4626 | 0.1003 |
| Eigenvalue | 1.2840 | 1.0836 | 0.8798 | 0.7527 |
| Variance % | 32.0995 | 27.0892 | 21.9941 | 18.8172 |
| Cumulative Variance % | 32.0995 | 59.1887 | 81.1828 | 100.0000 |

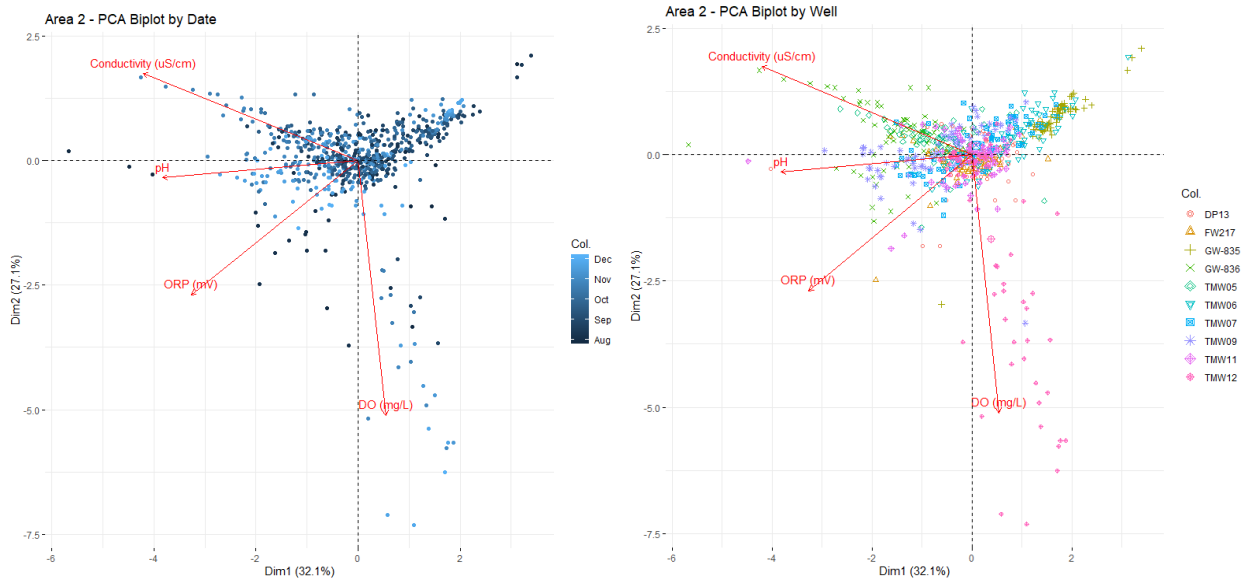


Figure 13: Area 2 PCA summary (top), PCA plot sorted by date (left) and well (right)

| Area 3 | PCA1 | PCA2 | PCA3 | PCA4 |
|------------------------------------------|----------------|----------------|----------------|-----------------|
| DO (mg/L) | 0.0967 | 0.5174 | 0.3834 | 0.0025 |
| ORP (mV) | 0.8287 | 0.0002 | 0.0127 | 0.1585 |
| Conductivity ($\mu\text{S}/\text{cm}$) | 0.0206 | 0.6337 | 0.3457 | 0.0000 |
| pH | 0.7999 | 0.0117 | 0.0380 | 0.1504 |
| Eigenvalue | 1.7458 | 1.1630 | 0.7799 | 0.3114 |
| Variance % | 43.6438 | 29.0740 | 19.4972 | 7.7851 |
| Cumulative Variance % | 43.6438 | 72.7178 | 92.2149 | 100.0000 |

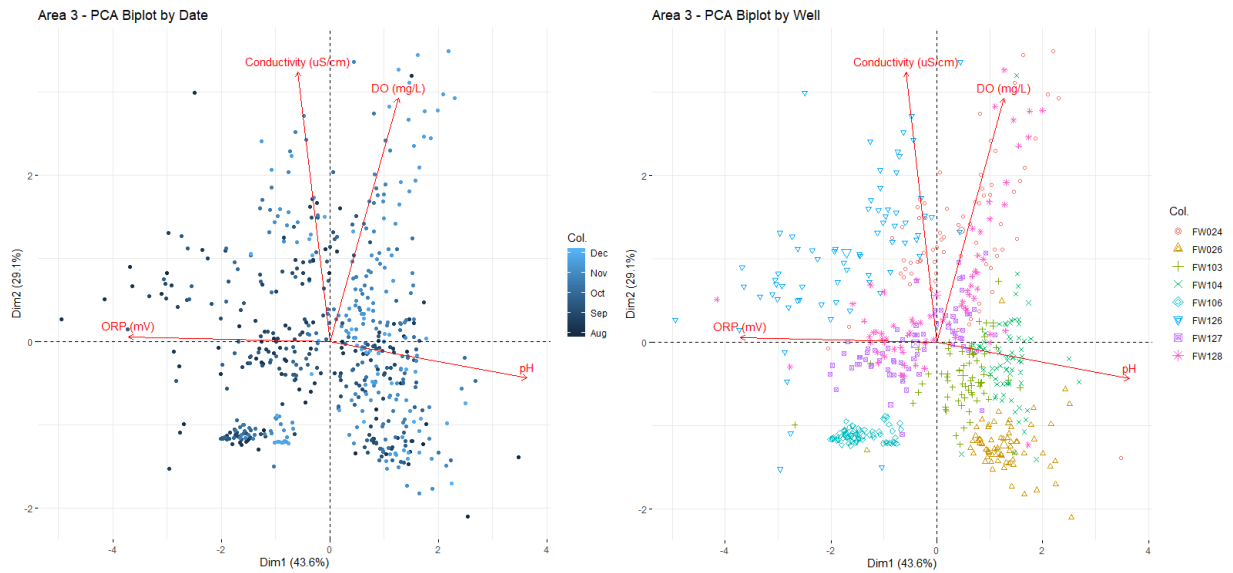


Figure 14: Area 3 PCA summary (*top*), PCA plot sorted by date (*left*) and well (*right*)

is a much larger range of PCA data points for Area 3 than the other areas, suggesting less outlier wells. This aligns with fact that Area 3 has the smallest footprint of the three areas. There is also less clustering in terms of time, with minor clusters before the dry season towards the ORP (to the left), and during wet conditions towards conductivity (upper-right). These results show that water table variations play less of a role on dominating geochemical parameters in the area. This, again, suggests that high nitrate contamination from the former S-3 Ponds is the largest governing force in determining these groundwater parameters.

5.0 Conclusions and Future Work

This work demonstrates the effect seasonal and short-term water table variations have on certain geochemical parameters in a timeseries framework. Specifically, results of the tested hypothesis over the timeseries indicate as follows:

- 1) Seasonal and short-term water table variations are expected to cause statistically significant changes in DO, conductivity, ORP, and pH in wells near the former S-3 ponds.

Null hypothesis rejected: In each area, wells exhibited significant changes in response to water table variations for the specific geochemical parameters measured.

- 2) Measurements from wells that are close to the initial water table are expected to show greater changes in parameters than deeper wells.

Failure to reject the null hypothesis: Overall, the deeper wells (12 to 14 m in Area 3) showed more significant changes in the measured geochemical parameters than more shallow wells (3 to 7.5 m in Areas 1 and 2).

- 3) Wells in highly contaminated groundwater zones are expected to respond differently to changes in water table than wells in less contaminated groundwater zones.

Null hypothesis rejected: Wells in highly contaminated groundwater zones (Area 3) showed different responses to water table variations than wells in less contaminated groundwater zones (Areas 1 and 2).

Trends showed that most wells in Areas 1 exhibited significant changes in DO and conductivity throughout the timeseries, while insignificant in ORP and pH. Overall, Area 2 wells had the least significant responses to water table variations. More wells in Area 3 responded significantly to water table fluctuations in ORP and pH than Areas 1 and 2. Area 3 wells are deeper and in a highly contaminated groundwater zone, while Areas 1 and 2 are shallower and in less contaminated groundwater areas.

PCA for each area also showed that water table variations play important roles in controlling certain geochemical parameters in wells downstream of the former S-3 Ponds. However, for areas in highly contaminated groundwater zones, PCA showed less outliers in measured parameters suggesting more stability over wells in less contaminated regions. These findings can be useful to researchers when planning to map geochemical parameters in certain areas. Knowing the potential effects water table variations have on specific geochemical

parameters can help researchers to work with or around weather and water table variations when developing a sampling plan.

This work also shows the ability to investigate levels of contamination with relatively few geochemical parameters based on water table variations over time. DO in highly contaminated groundwater did not exhibit the same patterns as less contaminated groundwater, even with the same climate exposure. This indicates that denitrification could be a major dominating process, while the fluctuating oxic conditions and higher DO and pH in Areas 1 and 2 suggest varying redox processes. These findings can be replicated to help researchers predict areas or plumes of groundwater contaminants and help identify source flow as well as underlying soil structure.

The next steps to further the discussion on this research is model validation through laboratory geochemical analysis. Once completed datasets for metals, anions, organic acids, and total organic carbon and nitrogen are produced, these data can help to identify and confirm the effects of water table variations and levels of contamination on microbial biodegradation tendencies in a dynamic groundwater environment over time.

Through this research, additional actions have been set up to examine in-depth, local stratigraphy using cone penetrometer technology to determine the role of local geology on groundwater and contaminant flow. New wells are also being established (specifically in Area 3) in hopes of examining groundwater processes in high contaminated groundwater and low contaminated within a small footprint (slightly above groundwater flow from the S-3 Ponds to directly in the contaminated plume). This, along with analysis of dominating functioning microbial communities, will allow researchers to examine highly contaminated soil and groundwater in a systems biology approach (18).

6.0 References

1. Grunsky E. 2010. The interpretation of geochemical survey data, vol 10.
2. Grunsky EC, Caritat Pd. 2019. State-of-the-art analysis of geochemical data for mineral exploration. *Geochemistry: Exploration, Environment, Analysis* doi:10.1144/geochem2019-031.
3. Reimann C, Matschullat J, Birke M, Salminen R. 2009. Arsenic distribution in the environment: The effects of scale. *Applied Geochemistry* 24:1147-1167.
4. Langwaldt JH, Puhakka JA. 2000. On-site biological remediation of contaminated groundwater: a review. *Environmental Pollution* 107:187-197.
5. Wang TA, McTernan WF. 2002. The development and application of a multilevel decision analysis model for the remediation of contaminated groundwater under uncertainty. *Journal of Environmental Management* 64:221-235.
6. Hashim MA, Mukhopadhyay S, Sahu JN, Sengupta B. 2011. Remediation technologies for heavy metal contaminated groundwater. *Journal of Environmental Management* 92:2355-2388.
7. Blowes DW, Ptacek CJ, Jambor JL. 1997. In-Situ Remediation of Cr(VI)-Contaminated Groundwater Using Permeable Reactive Walls: Laboratory Studies. *Environmental Science & Technology* 31:3348-3357.
8. Yeung AT, Gu Y-Y. 2011. A review on techniques to enhance electrochemical remediation of contaminated soils. *Journal of Hazardous Materials* 195:11-29.
9. Haugen KS, Semmens MJ, Novak PJ. 2002. A novel in situ technology for the treatment of nitrate contaminated groundwater. *Water Research* 36:3497-3506.
10. Naudet V, Rizzo E, Bottero J-Y, Bégassat P. 2004. Groundwater redox conditions and conductivity in a contaminant plume from geoelectrical investigations. *Hydrology and Earth System Sciences* 8.
11. Haberer CM, Rolle M, Cirpka OA, Grathwohl P. 2012. Oxygen Transfer in a Fluctuating Capillary Fringe. *Vadose Zone Journal* 11.
12. Rezanezhad F, Couture R-M, Kovac R, O'Connell D, Van Cappellen P. 2014. Water Table Fluctuations and Soil Biogeochemistry: An Experimental Approach Using an Automated Soil Column System, vol 509.
13. Haberer CM, Rolle M, Cirpka OA, Grathwohl P. 2015. Impact of Heterogeneity on Oxygen Transfer in a Fluctuating Capillary Fringe. *Groundwater* 53:57-70.
14. Jost D, M. Haberer C, Grathwohl P, Winter J, Gallert C. 2014. Oxygen Transfer in a Fluctuating Capillary Fringe: Impact of Microbial Respiratory Activity, vol 0.
15. Korom SF. 1992. Natural denitrification in the saturated zone: A review. *Water Resources Research* 28:1657-1668.
16. Rivett MO, Buss SR, Morgan P, Smith JWN, Bemment CD. 2008. Nitrate attenuation in groundwater: A review of biogeochemical controlling processes. *Water Research* 42:4215-4232.
17. Harte PT, Ayotte J, Hoffman A, Révész K, Belaval M, Lamb S, Bohlke J. 2012. Heterogeneous redox conditions, arsenic mobility, and groundwater flow in fractured-rock aquifer near a waste repository site in New Hampshire, USA. *Hydrogeology Journal* 20:1189–1201.

18. Hazen TC. 2019. Environmental Systems Biology Approach to Bioremediation, p 103-127. *In* Hurst CJ (ed), Understanding Terrestrial Microbial Communities doi:10.1007/978-3-030-10777-2_4. Springer International Publishing, Cham.
19. Hazen TC. 2018. In Situ: Groundwater Bioremediation, p 1-18. *In* Steffan R (ed), Consequences of Microbial Interactions with Hydrocarbons, Oils, and Lipids: Biodegradation and Bioremediation doi:10.1007/978-3-319-44535-9_11-1. Springer International Publishing, Cham.
20. McMahon PB, Chapelle FH. 2008. Redox Processes and Water Quality of Selected Principal Aquifer Systems. *Groundwater* 46:259-271.
21. Smedley PL, Kinniburgh DG. 2002. A review of the source, behaviour and distribution of arsenic in natural waters. *Applied Geochemistry* 17:517-568.
22. Christensen TH, Bjerg PL, Banwart SA, Jakobsen R, Heron G, Albrechtsen H-J. 2000. Characterization of redox conditions in groundwater contaminant plumes. *Journal of Contaminant Hydrology* 45:165-241.
23. Kerfoot H. 1994. In Situ Determination of the Rate of Unassisted Degradation of Saturated-Zone Hydrocarbon Contamination, vol 44.
24. Lee C-H, Lee J-Y, Cheon J-Y, Lee K-K. 2001. Attenuation of Petroleum Hydrocarbons in Smear Zones: A Case Study, vol 127.
25. Gavrilesco M. 2006. Overview of in situ remediation technologies for sites and groundwater. *Environmental Engineering and Management Journal*; Vol 5, No 1 (2006).
26. Subramani T, Rajmohan N, Elango L. 2010. Groundwater geochemistry and identification of hydrogeochemical processes in a hard rock region, Southern India. *Environmental Monitoring and Assessment* 162:123-137.
27. Dickopp J, Lengerer A, Kazda M. 2018. Relationship between groundwater levels and oxygen availability in fen peat soils. *Ecological Engineering* 120:85-93.
28. Islam J, Singhal N, O'Sullivan M. 2001. Modeling Biogeochemical Processes in Leachate-Contaminated Soils: A Review, vol 43.
29. Jost D, Winter J, Gallert C. 2011. Water and Oxygen Dependence of Growing in Silica Sand Capillary Fringes, vol 10.
30. Williams XK. 1967. Statistics in the interpretation of geochemical data. *New Zealand Journal of Geology and Geophysics* 10:771-797.
31. Mukherjee A, von Brömssen M, Scanlon BR, Bhattacharya P, Fryar AE, Hasan MA, Ahmed KM, Chatterjee D, Jacks G, Sracek O. 2008. Hydrogeochemical comparison and effects of overlapping redox zones on groundwater arsenic near the Western (Bhagirathi sub-basin, India) and Eastern (Meghna sub-basin, Bangladesh) margins of the Bengal Basin. *Journal of Contaminant Hydrology* 99:31-48.
32. Lee J-J, Jang C-S, Wang S-W, Liang C-P, Liu C-W. 2008. Delineation of spatial redox zones using discriminant analysis and geochemical modelling in arsenic-affected alluvial aquifers. *Hydrological Processes* 22:3029-3041.
33. Rainwater K, Mayfield MP, Heintz C, Claborn BJ. 1993. Enhanced in situ biodegradation of diesel fuel by cyclic vertical water table movement: preliminary studies. *Water Environment Research* 65:717-725.
34. Amos RT, Ulrich Mayer K. 2006. Investigating the role of gas bubble formation and entrapment in contaminated aquifers: Reactive transport modelling. *Journal of Contaminant Hydrology* 87:123-154.

35. M Haberer C, Rolle M, Liu S, Cirpka O, Grathwohl P. 2011. A high-resolution non-invasive approach to quantify oxygen transport across the capillary fringe and within the underlying groundwater, vol 122.
36. Dobson R, Schroth MH, Zeyer J. 2007. Effect of water-table fluctuation on dissolution and biodegradation of a multi-component, light nonaqueous-phase liquid. *Journal of Contaminant Hydrology* 94:235-248.
37. Haberer CM, Rolle M, Cirpka OA, Grathwohl P. 2012. Oxygen Transfer in a Fluctuating Capillary Fringe. *Vadose Zone Journal* 11:vzj2011.0056.
38. Luo J, Kurt Z, Hou D, Spain JC. 2015. Modeling Aerobic Biodegradation in the Capillary Fringe. *Environmental Science & Technology* 49:1501-1510.
39. Deng Y, Li H, Wang Y, Duan Y, Gan Y. 2014. Temporal Variability of Groundwater Chemistry and Relationship with Water-table Fluctuation in the Jiangnan Plain, Central China. *Procedia Earth and Planetary Science* 10:100-103.
40. Rezanezhad F, Couture RM, Kovac R, O'Connell D, Van Cappellen P. 2014. Water table fluctuations and soil biogeochemistry: An experimental approach using an automated soil column system. *Journal of Hydrology* 509:245-256.
41. Jost D, Haberer CM, Grathwohl P, Winter J, Gallert C. 2015. Oxygen Transfer in a Fluctuating Capillary Fringe: Impact of Microbial Respiratory Activity. *Vadose Zone Journal* 14:vzj2014.04.0039.
42. Werner D, Höhener P. 2002. The influence of water table fluctuations on the volatilization of contaminants from groundwater.
43. D Klenk I, Grathwohl P. 2002. Transverse vertical dispersion in groundwater and the capillary fringe, vol 58.
44. Sinke AJC, Dury O, Zobrist J. 1998. Effects of a fluctuating water table: column study on redox dynamics and fate of some organic pollutants. *Journal of Contaminant Hydrology* 33:231-246.
45. Anonymous. 1993. Remedial investigation work plan for Bear Creek Valley Operable Unit 1 (S-3 Ponds, Boneyard/Burnyard, Oil Landfarm, Sanitary Landfill 1, and the Burial Grounds, including Oil Retention Ponds 1 and 2) at the Oak Ridge Y-12 Plant, Oak Ridge, Tennessee. Volume 1, Main text. United States.
46. Anonymous. 1996. Report on the remedial investigation of Bear Creek Valley at the Oak Ridge Y-12 Plant, Oak Ridge, Tennessee. Volume 3: Appendix D -- Nature and extent of contamination report. United States.
47. Phillips DH, Gu B, Watson DB, Roh Y, Liang L, Lee SY. 2000. Performance Evaluation of a Zerovalent Iron Reactive Barrier: Mineralogical Characteristics. *Environmental Science & Technology* 34:4169-4176.
48. Phillips DH, Watson DB, Roh Y, Gu B. 2003. Mineralogical Characteristics and Transformations during Long-Term Operation of a Zerovalent Iron Reactive Barrier. *Journal of Environmental Quality* 32:2033-2045.
49. Henderson AD, Demond AH. 2007. Long-Term Performance of Zero-Valent Iron Permeable Reactive Barriers: A Critical Review. *Environmental Engineering Science* 24:401-423.
50. Rockworks. 2017. Rockworks 17 Training Manual. Rockware, Colorado.
51. Sakata S, Ashida F, Zako M. 2004. An efficient algorithm for Kriging approximation and optimization with large-scale sampling data. *Computer Methods in Applied Mechanics and Engineering* 193:385-404.

52. Rossi RE, Dungan JL, Beck LR. 1994. Kriging in the shadows: Geostatistical interpolation for remote sensing. *Remote Sensing of Environment* 49:32-40.
53. RStudio Team (2020). RStudio: Integrated Development for R. RStudio P, Boston, MA URL <http://www.rstudio.com/>.
54. Weinfurt KP. 1995. Multivariate analysis of variance, p 245-276. American Psychological Association, Washington, DC, US.
55. Huberty CJ, Petoskey MD. 2000. 7 - Multivariate Analysis of Variance and Covariance, p 183-208. In Tinsley HEA, Brown SD (ed), *Handbook of Applied Multivariate Statistics and Mathematical Modeling* doi:<https://doi.org/10.1016/B978-012691360-6/50008-2>. Academic Press, San Diego.
56. Wickham H. 2016. *ggplot2: Elegant Graphics for Data Analysis*, Springer-Verlag New York.
57. Novomestky LKaF. 2015. moments: Moments, cumulants, skewness, kurtosis and related tests. R package version 0.14, p <https://CRAN.R-project.org/package=moments>.
58. Wold S, Esbensen K, Geladi P. 1987. Principal component analysis. *Chemometrics and Intelligent Laboratory Systems* 2:37-52.
59. Abdi H, Williams LJ. 2010. Principal component analysis. *WIREs Computational Statistics* 2:433-459.
60. Helena B, Pardo R, Vega M, Barrado E, Fernandez JM, Fernandez L. 2000. Temporal evolution of groundwater composition in an alluvial aquifer (Pisuerga River, Spain) by principal component analysis. *Water Research* 34:807-816.
61. Belkhiri L, Boudoukha A, Mouni L. 2011. A multivariate statistical analysis of groundwater chemistry data. *International Journal of Environmental Research (IJER)* 5:537-544.
62. Mundt AKaF. 2020. factoextra: Extract and Visualize the Results of Multivariate Data Analyses. R package version 1.0.7.
63. Joyner WTaDA. 2019. September 2019 Tennessee State Climate Summary. Tennessee Climate Office * East Tennessee State University with contributions by Climate Data Representatives at University of Tennessee-Martin, Vanderbilt University, and University of Tennessee-Institute of Agriculture,
64. Joyner WTaDA. 2019. October 2019 Tennessee State Climate Summary. Tennessee Climate Office * East Tennessee State University with contributions by Climate Data Representatives at University of Tennessee-Martin, Vanderbilt University, and University of Tennessee-Institute of Agriculture,
65. Mohamed MAA, Terao H, Suzuki R, Babiker IS, Ohta K, Kaori K, Kato K. 2003. Natural denitrification in the Kakamigahara groundwater basin, Gifu prefecture, central Japan. *Science of The Total Environment* 307:191-201.
66. Charlson RJ, Rodhe H. 1982. Factors controlling the acidity of natural rainwater. *Nature* 295:683-685.
67. Liljestrand HM. 1985. Average rainwater pH, concepts of atmospheric acidity, and buffering in open systems. *Atmospheric Environment (1967)* 19:487-499.
68. Castro MC, Goblet P. 2003. Calibration of regional groundwater flow models: Working toward a better understanding of site-specific systems. *Water Resources Research* 39.

Appendix A: Areas Downstream of the former S-3 Ponds



Figure 15: Area 1 Wells

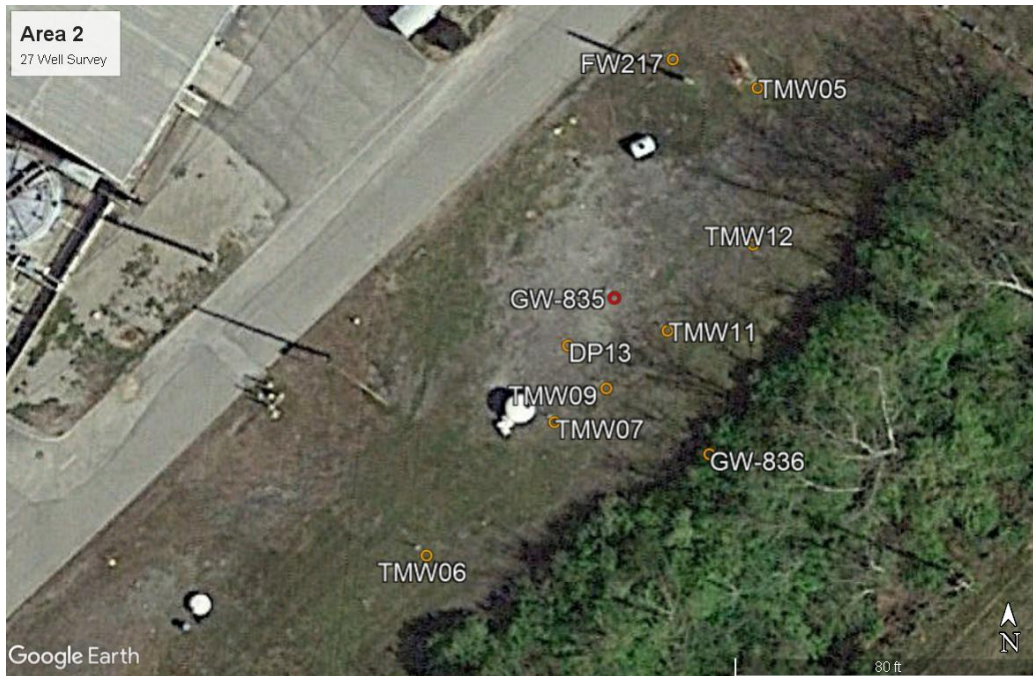


Figure 16: Area 2 Wells

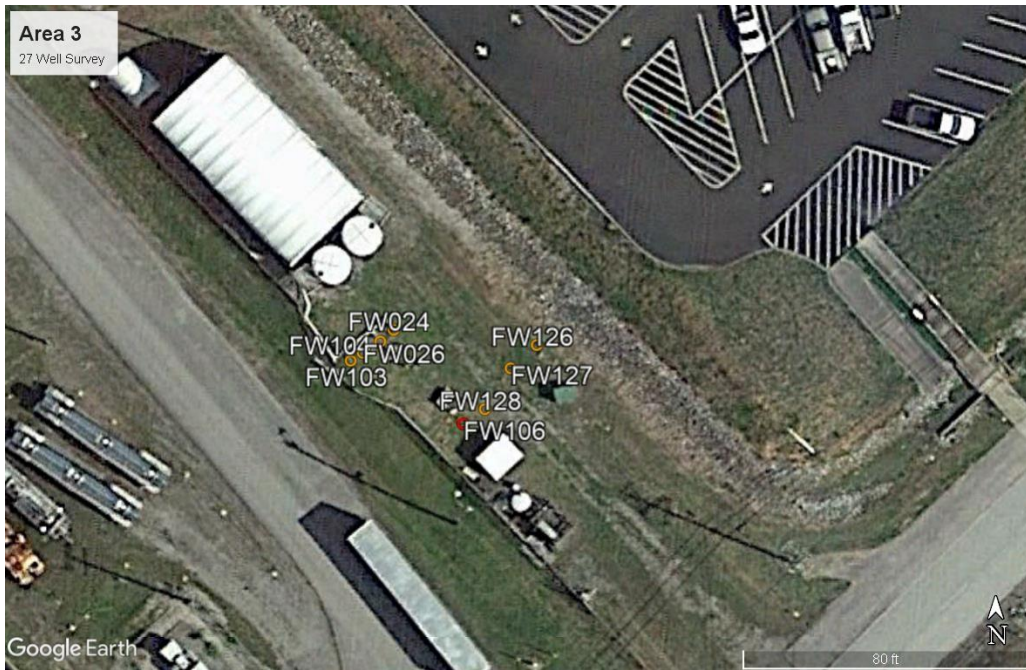


Figure 17: Area 3 Wells

Appendix B: Summary Statistics

Table 3: Area 1 Summary Statistics

| Parameter | | DO (mg/L) | ORP (mV) | Conductivity (μ S/cm) | pH | Water Elevation (m AMSL) |
|-----------|--------------------|-----------|----------|-------------------------------|------|--------------------------------|
| EU02 | MIN | 0.00 | 185.29 | 684.23 | 6.44 | 303.18 |
| | MAX | 1.69 | 583.98 | 2069.13 | 7.37 | 304.35 |
| | Mean | 0.41 | 233.70 | 1095.28 | 6.94 | 303.71 |
| | Median | 0.28 | 220.09 | 1043.56 | 6.94 | 303.78 |
| | Standard Deviation | 0.36 | 55.44 | 262.47 | 0.19 | 0.33 |
| EU03 | MIN | 0.33 | 174.60 | 548.76 | 6.58 | 303.16 |
| | MAX | 5.37 | 557.13 | 1711.39 | 7.47 | 304.31 |
| | Mean | 1.84 | 233.95 | 1134.85 | 7.00 | 303.70 |
| | Median | 0.91 | 219.27 | 1091.78 | 6.98 | 303.76 |
| | Standard Deviation | 1.67 | 53.86 | 237.15 | 0.17 | 0.32 |
| ED04 | MIN | 0.10 | 143.70 | 456.04 | 6.74 | 303.23 |
| | MAX | 5.46 | 546.54 | 1719.15 | 7.57 | 304.37 |
| | Mean | 0.92 | 231.23 | 910.21 | 7.14 | 303.76 |
| | Median | 0.25 | 217.99 | 876.31 | 7.11 | 303.81 |
| | Standard Deviation | 1.30 | 56.11 | 225.79 | 0.15 | 0.32 |
| EU05 | MIN | 0.00 | -159.59 | 698.56 | 6.89 | 303.17 |
| | MAX | 4.60 | 243.94 | 883.45 | 7.09 | 304.32 |
| | Mean | 1.02 | 119.67 | 763.47 | 6.98 | 303.69 |
| | Median | 0.08 | 155.77 | 747.06 | 6.97 | 303.73 |
| | Standard Deviation | 1.46 | 93.72 | 48.59 | 0.06 | 0.33 |
| ED06 | MIN | 0.00 | 196.08 | 526.98 | 6.61 | 303.23 |
| | MAX | 3.08 | 515.97 | 1559.72 | 7.90 | 304.38 |
| | Mean | 0.62 | 269.51 | 955.80 | 7.17 | 303.76 |
| | Median | 0.28 | 260.02 | 924.16 | 7.17 | 303.82 |
| | Standard Deviation | 0.75 | 51.30 | 211.83 | 0.25 | 0.33 |
| EU07 | MIN | 0.97 | 113.32 | 445.58 | 6.41 | 303.13 |
| | MAX | 8.27 | 517.72 | 1508.28 | 7.74 | 304.29 |
| | Mean | 2.83 | 287.43 | 860.95 | 7.03 | 303.69 |
| | Median | 2.32 | 284.01 | 814.67 | 7.01 | 303.75 |
| | Standard Deviation | 1.49 | 60.29 | 205.89 | 0.29 | 0.33 |
| ED08 | MIN | 0.05 | 111.24 | 526.14 | 6.60 | 303.23 |
| | MAX | 2.37 | 457.18 | 1563.92 | 7.89 | 304.34 |
| | Mean | 0.28 | 250.81 | 915.49 | 7.19 | 303.76 |
| | Median | 0.15 | 249.02 | 854.50 | 7.17 | 303.83 |
| | Standard Deviation | 0.40 | 74.97 | 216.16 | 0.24 | 0.32 |
| FW065 | MIN | 0.00 | 89.24 | 537.85 | 2.84 | 303.04 |
| | MAX | 4.54 | 434.23 | 7733.19 | 7.41 | 304.01 |
| | Mean | 1.07 | 209.21 | 2819.51 | 6.16 | 303.47 |
| | Median | 0.66 | 201.63 | 2192.06 | 6.07 | 303.51 |
| | Standard Deviation | 1.05 | 56.42 | 1810.33 | 0.74 | 0.24 |
| FW066 | MIN | 0.00 | 104.58 | 1132.25 | 5.29 | 302.99 |
| | MAX | 3.56 | 463.54 | 4617.29 | 7.11 | 303.97 |
| | Mean | 0.67 | 203.83 | 2496.48 | 6.31 | 303.46 |
| | Median | 0.26 | 191.51 | 2353.02 | 6.25 | 303.53 |
| | Standard Deviation | 0.91 | 54.38 | 635.28 | 0.34 | 0.26 |

Table 4: Area 2 Summary Statistics

| Parameter | | DO (mg/L) | ORP (mV) | Conductivity ($\mu\text{S}/\text{cm}$) | pH | Water Elevation (m AMSL) |
|-----------|--------------------|-----------|----------|---------------------------------------------|-------|--------------------------------|
| DP13 | MIN | 0.00 | 83.31 | 200.19 | 6.68 | 303.18 |
| | MAX | 1.47 | 458.61 | 1754.52 | 9.77 | 304.35 |
| | Mean | 0.34 | 184.41 | 960.43 | 7.06 | 303.71 |
| | Median | 0.20 | 162.07 | 946.10 | 6.99 | 303.78 |
| | Standard Deviation | 0.34 | 64.56 | 279.80 | 0.37 | 0.33 |
| FW217 | MIN | 0.07 | 23.50 | 265.01 | 6.62 | 303.16 |
| | MAX | 0.35 | 575.32 | 2209.45 | 7.37 | 304.31 |
| | Mean | 0.19 | 218.00 | 1088.83 | 7.04 | 303.70 |
| | Median | 0.19 | 212.91 | 1057.37 | 7.03 | 303.76 |
| | Standard Deviation | 0.06 | 62.03 | 309.38 | 0.16 | 0.32 |
| GW-835 | MIN | 0.00 | -131.88 | 710.25 | 6.34 | 303.23 |
| | MAX | 3.95 | 268.83 | 2283.46 | 6.86 | 304.37 |
| | Mean | 0.06 | 94.93 | 936.83 | 6.55 | 303.76 |
| | Median | 0.00 | 98.79 | 859.67 | 6.58 | 303.81 |
| | Standard Deviation | 0.47 | 55.60 | 230.51 | 0.11 | 0.32 |
| GW-836 | MIN | 0.00 | 91.81 | 1621.81 | 6.63 | 303.17 |
| | MAX | 2.52 | 438.16 | 4927.71 | 10.08 | 304.32 |
| | Mean | 0.56 | 197.14 | 2768.17 | 7.10 | 303.69 |
| | Median | 0.30 | 180.52 | 2667.44 | 7.02 | 303.73 |
| | Standard Deviation | 0.62 | 55.10 | 654.29 | 0.41 | 0.33 |
| TMW05 | MIN | 0.01 | 90.35 | 698.24 | 6.60 | 303.23 |
| | MAX | 1.38 | 448.98 | 3216.85 | 7.40 | 304.38 |
| | Mean | 0.12 | 213.94 | 1765.88 | 7.01 | 303.76 |
| | Median | 0.10 | 211.78 | 1707.28 | 7.01 | 303.82 |
| | Standard Deviation | 0.16 | 47.60 | 423.42 | 0.18 | 0.33 |
| TMW06 | MIN | 0.00 | -156.94 | 276.51 | 6.71 | 303.13 |
| | MAX | 0.36 | 266.90 | 1092.51 | 7.94 | 304.29 |
| | Mean | 0.11 | 112.35 | 584.98 | 7.19 | 303.69 |
| | Median | 0.09 | 111.32 | 548.92 | 7.16 | 303.75 |
| | Standard Deviation | 0.09 | 89.05 | 161.50 | 0.22 | 0.33 |
| TMW07 | MIN | 0.00 | 30.96 | 626.00 | 6.64 | 303.23 |
| | MAX | 0.39 | 370.00 | 1846.99 | 7.78 | 304.34 |
| | Mean | 0.13 | 170.00 | 1049.12 | 7.13 | 303.76 |
| | Median | 0.12 | 160.94 | 982.42 | 7.13 | 303.83 |
| | Standard Deviation | 0.09 | 78.99 | 242.62 | 0.21 | 0.32 |
| TMW09 | MIN | 0.03 | 35.14 | 388.11 | 6.93 | 303.04 |
| | MAX | 3.82 | 359.96 | 2254.32 | 7.99 | 304.01 |
| | Mean | 0.22 | 198.51 | 1312.94 | 7.34 | 303.47 |
| | Median | 0.16 | 206.99 | 1268.56 | 7.34 | 303.51 |
| | Standard Deviation | 0.45 | 74.86 | 314.49 | 0.20 | 0.24 |
| TMW11 | MIN | 0.00 | 87.46 | 676.29 | 6.73 | 302.99 |
| | MAX | 1.77 | 480.23 | 2003.23 | 9.91 | 303.97 |
| | Mean | 0.43 | 184.10 | 1110.89 | 7.13 | 303.46 |
| | Median | 0.27 | 166.01 | 1063.74 | 7.06 | 303.53 |
| | Standard Deviation | 0.44 | 62.18 | 263.77 | 0.38 | 0.26 |
| TMW12 | MIN | 0.06 | 130.59 | 176.45 | 6.61 | 13.30 |
| | MAX | 8.61 | 469.34 | 1416.43 | 7.57 | 15.20 |
| | Mean | 1.97 | 217.29 | 847.65 | 6.98 | 14.20 |
| | Median | 0.20 | 213.65 | 920.76 | 6.99 | 14.14 |
| | Standard Deviation | 2.52 | 46.13 | 362.28 | 0.18 | 0.40 |

Table 5: Area 3 Summary Statistics

| Parameter | | DO (mg/L) | ORP (mV) | Conductivity ($\mu\text{S}/\text{cm}$) | pH | Water Elevation (m AMSL) |
|-----------|--------------------|-----------|----------|---------------------------------------------|------|--------------------------------|
| FW024 | MIN | 0.00 | 58.94 | 7362.96 | 4.00 | 303.23 |
| | MAX | 0.98 | 444.88 | 26193.40 | 6.45 | 304.17 |
| | Mean | 0.40 | 271.42 | 13967.56 | 4.91 | 303.69 |
| | Median | 0.36 | 263.45 | 12980.10 | 4.94 | 303.78 |
| | Standard Deviation | 0.18 | 61.07 | 4120.06 | 0.42 | 0.25 |
| FW026 | MIN | 0.03 | 110.73 | 516.31 | 4.83 | 303.22 |
| | MAX | 0.32 | 424.86 | 17427.90 | 6.93 | 304.18 |
| | Mean | 0.10 | 235.63 | 4015.87 | 5.67 | 303.69 |
| | Median | 0.09 | 238.62 | 3846.18 | 5.62 | 303.74 |
| | Standard Deviation | 0.06 | 37.12 | 2205.06 | 0.40 | 0.26 |
| FW103 | MIN | 0.07 | 148.84 | 2631.84 | 4.09 | 303.17 |
| | MAX | 0.48 | 500.62 | 12881.80 | 5.59 | 304.12 |
| | Mean | 0.21 | 260.99 | 6289.00 | 4.99 | 303.63 |
| | Median | 0.20 | 261.77 | 5729.15 | 5.08 | 303.70 |
| | Standard Deviation | 0.07 | 41.94 | 2219.13 | 0.37 | 0.26 |
| FW104 | MIN | 0.05 | 86.00 | 70.93 | 4.95 | 303.14 |
| | MAX | 1.14 | 393.02 | 22885.50 | 6.38 | 304.07 |
| | Mean | 0.14 | 233.13 | 11281.91 | 5.79 | 303.59 |
| | Median | 0.12 | 235.68 | 10816.45 | 5.81 | 303.68 |
| | Standard Deviation | 0.13 | 39.59 | 3892.14 | 0.31 | 0.25 |
| FW106 | MIN | 0.00 | 267.42 | 5117.95 | 3.88 | 303.11 |
| | MAX | 0.05 | 387.92 | 8125.07 | 4.21 | 304.02 |
| | Mean | 0.01 | 335.21 | 5935.65 | 4.02 | 303.53 |
| | Median | 0.01 | 344.05 | 5807.68 | 4.02 | 303.59 |
| | Standard Deviation | 0.01 | 34.29 | 635.60 | 0.09 | 0.24 |
| FW126 | MIN | 0.00 | 186.12 | 45.39 | 2.72 | 303.12 |
| | MAX | 0.75 | 578.58 | 36942.00 | 5.14 | 304.02 |
| | Mean | 0.12 | 369.65 | 20406.74 | 4.16 | 303.56 |
| | Median | 0.10 | 358.81 | 20002.25 | 4.29 | 303.65 |
| | Standard Deviation | 0.11 | 81.86 | 6471.63 | 0.50 | 0.25 |
| FW127 | MIN | 0.09 | 184.64 | 583.10 | 3.82 | 302.86 |
| | MAX | 0.28 | 452.10 | 19301.10 | 5.47 | 304.06 |
| | Mean | 0.18 | 311.86 | 10124.53 | 4.67 | 303.61 |
| | Median | 0.17 | 319.24 | 9633.42 | 4.73 | 303.71 |
| | Standard Deviation | 0.04 | 67.02 | 3378.45 | 0.33 | 0.27 |
| FW128 | MIN | 0.00 | 136.96 | 7408.63 | 3.51 | 303.05 |
| | MAX | 0.92 | 619.31 | 22664.00 | 5.51 | 303.99 |
| | Mean | 0.24 | 265.87 | 12672.81 | 4.57 | 303.50 |
| | Median | 0.16 | 254.86 | 12322.45 | 4.67 | 303.57 |
| | Standard Deviation | 0.20 | 73.00 | 2946.06 | 0.45 | 0.24 |

Appendix C: Geochemical Parameters and Water Table Elevations

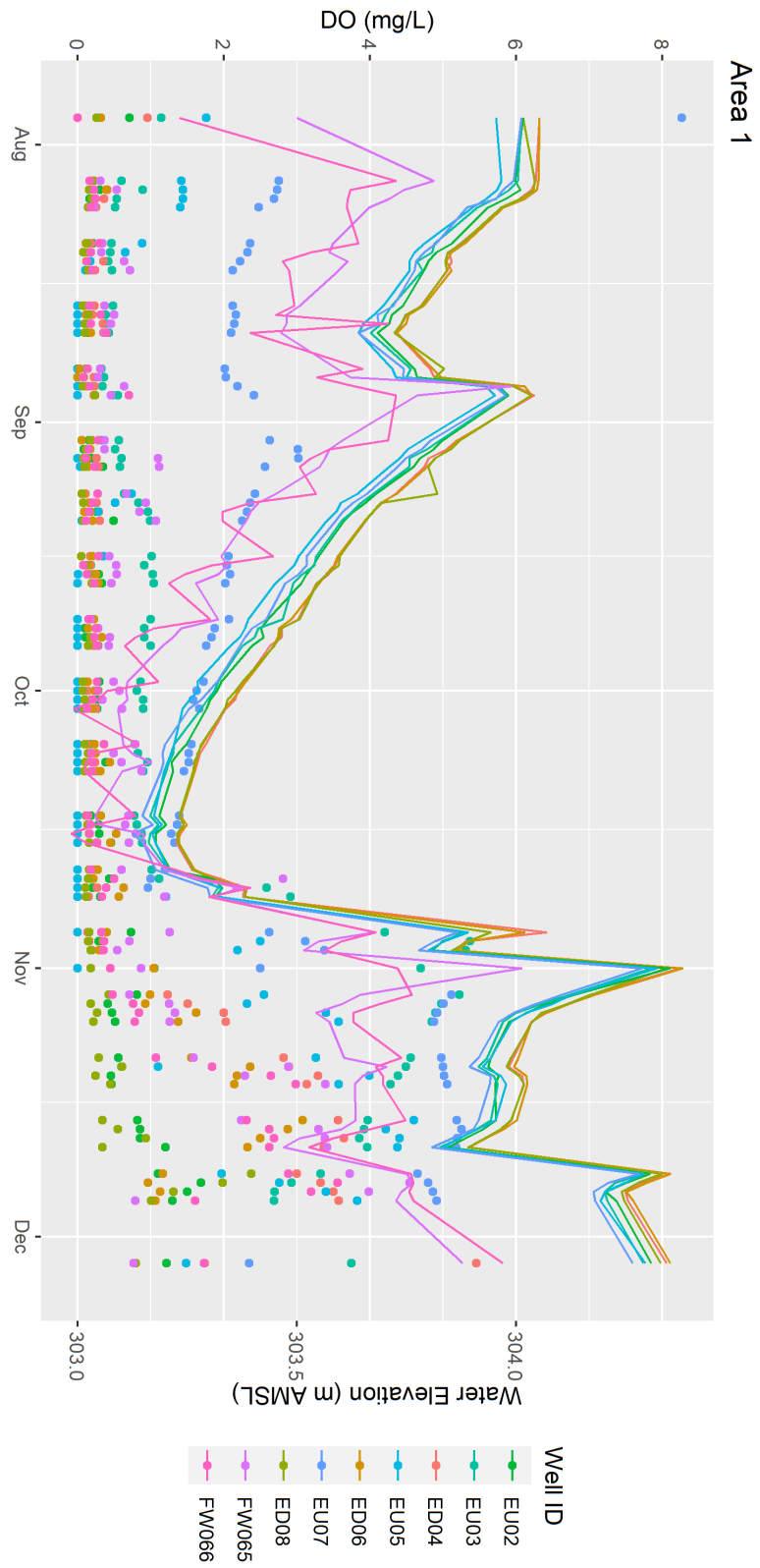


Figure 18: Area 1 – Dissolved oxygen in mg/L (points) and water table elevation in m AMSL (lines)

Area 1

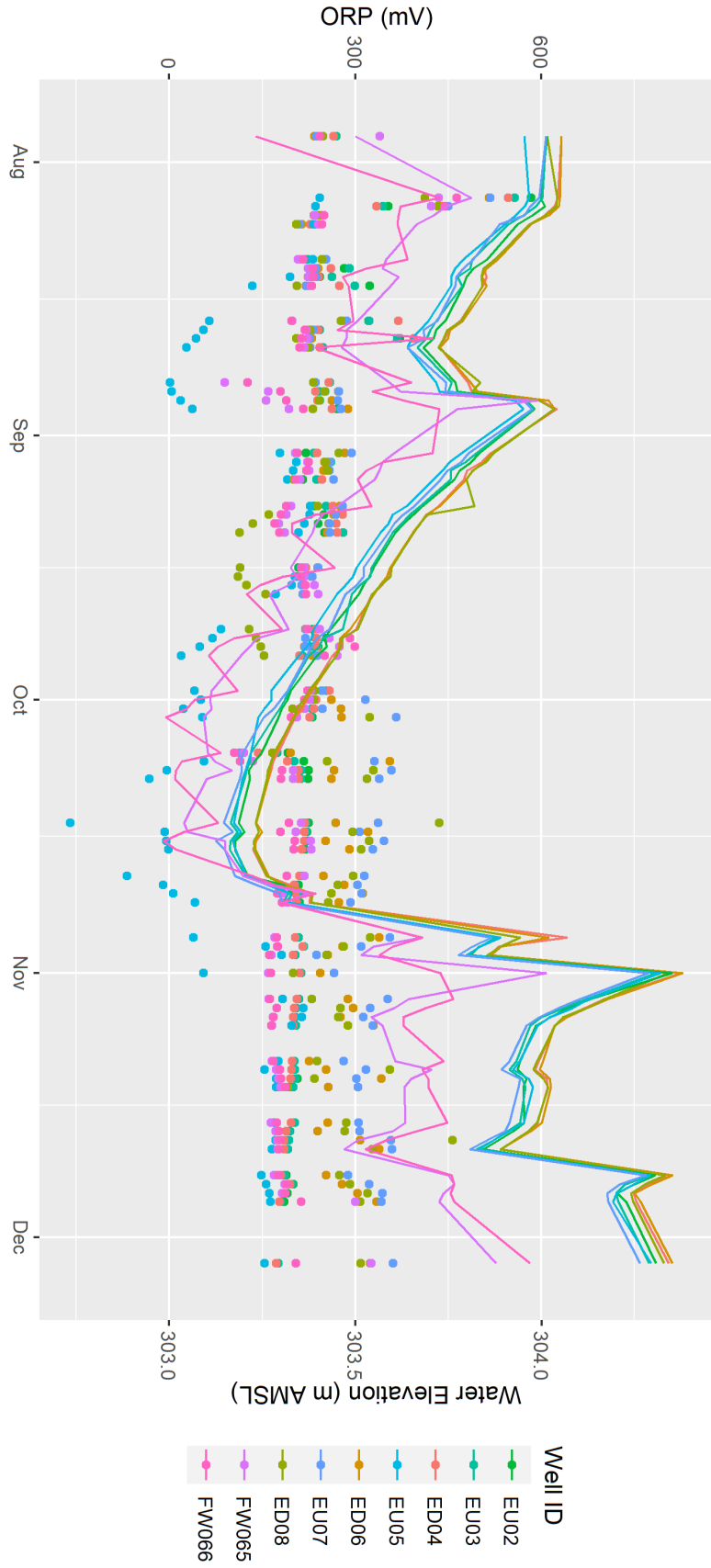


Figure 19: Area 1 – Oxidation-reduction potential in mV (points) and water table elevation in m AMSL (lines)

Area 1

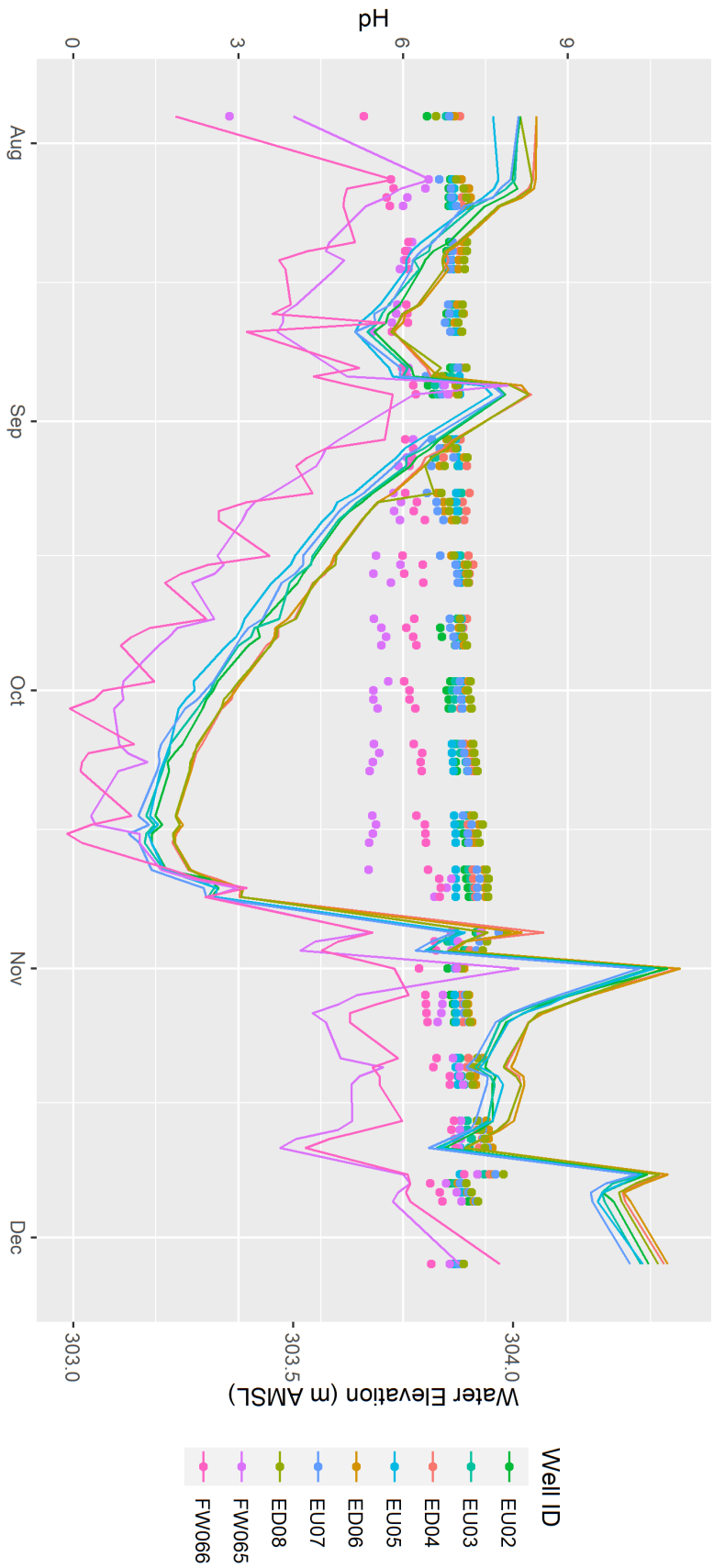


Figure 20: Area 1 – pH (points) and water table elevation in m AMSL (lines)

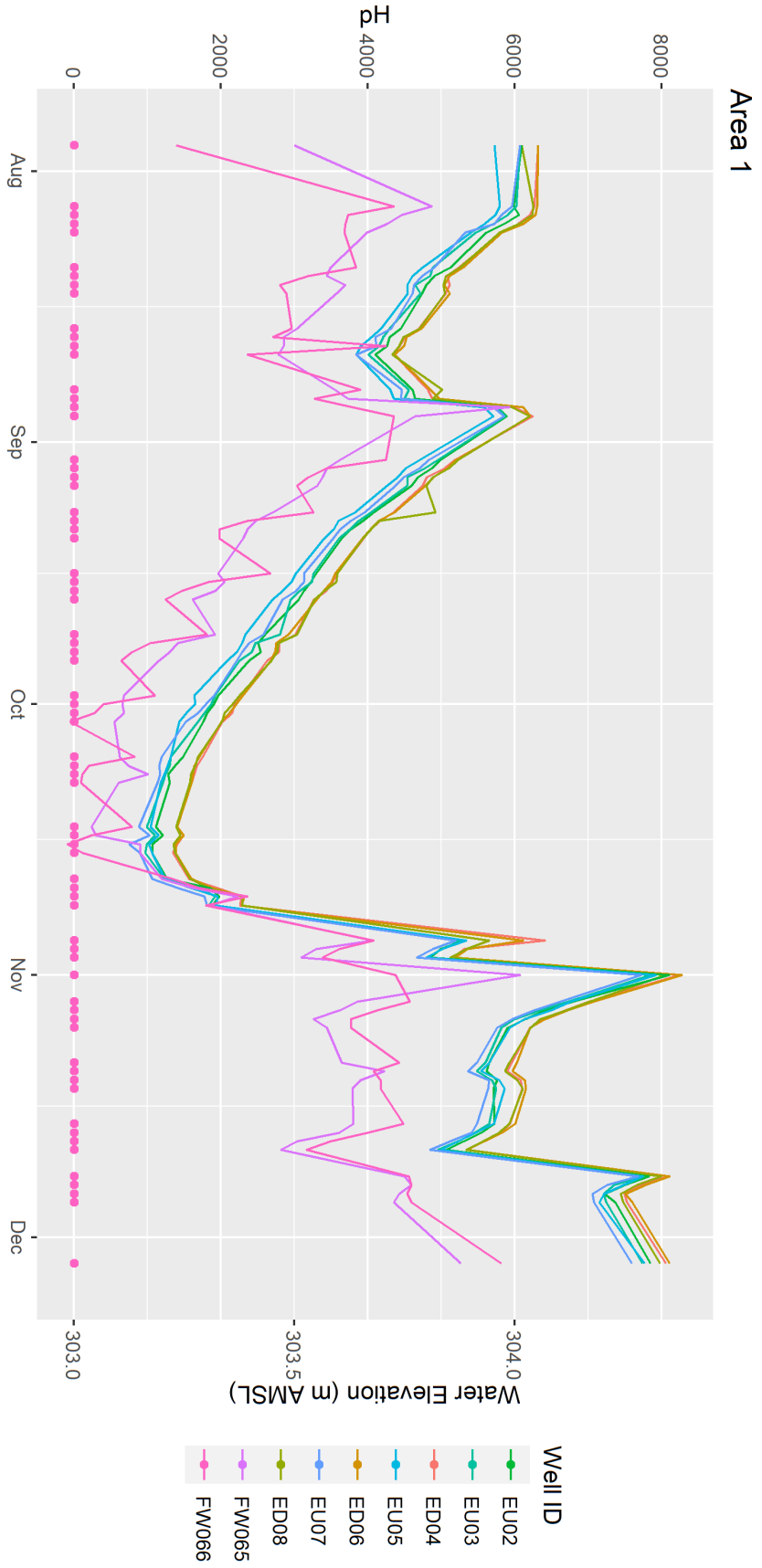


Figure 21: Area 1 – Specific Conductivity in µS/cm (points) and water table elevation in m AMSL (lines)

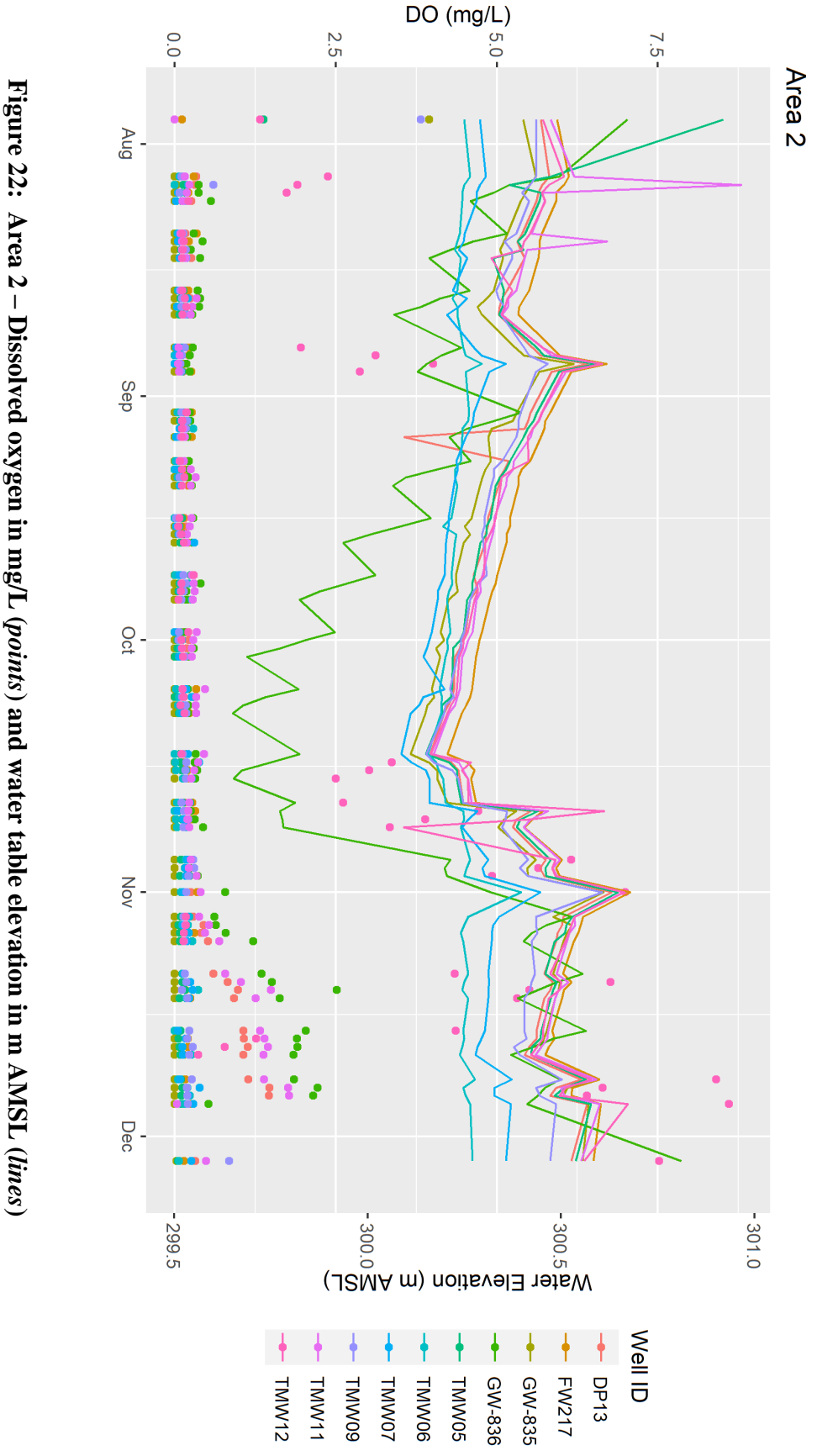


Figure 22: Area 2 – Dissolved oxygen in mg/L (points) and water table elevation in m AMSL (lines)

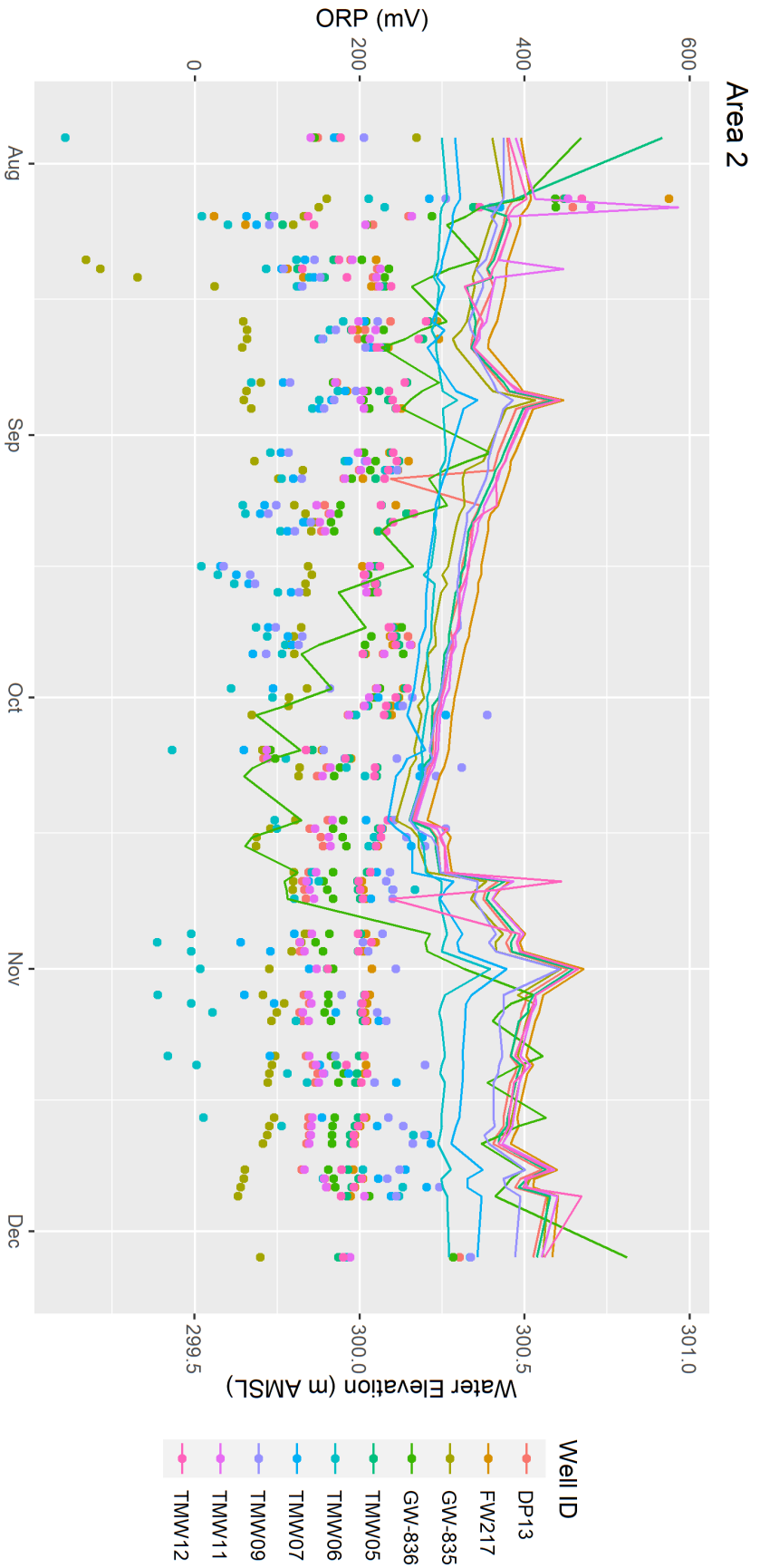


Figure 23: Area 2 – Oxidation-reduction potential in mV (points) and water table elevation in m AMSL (lines)

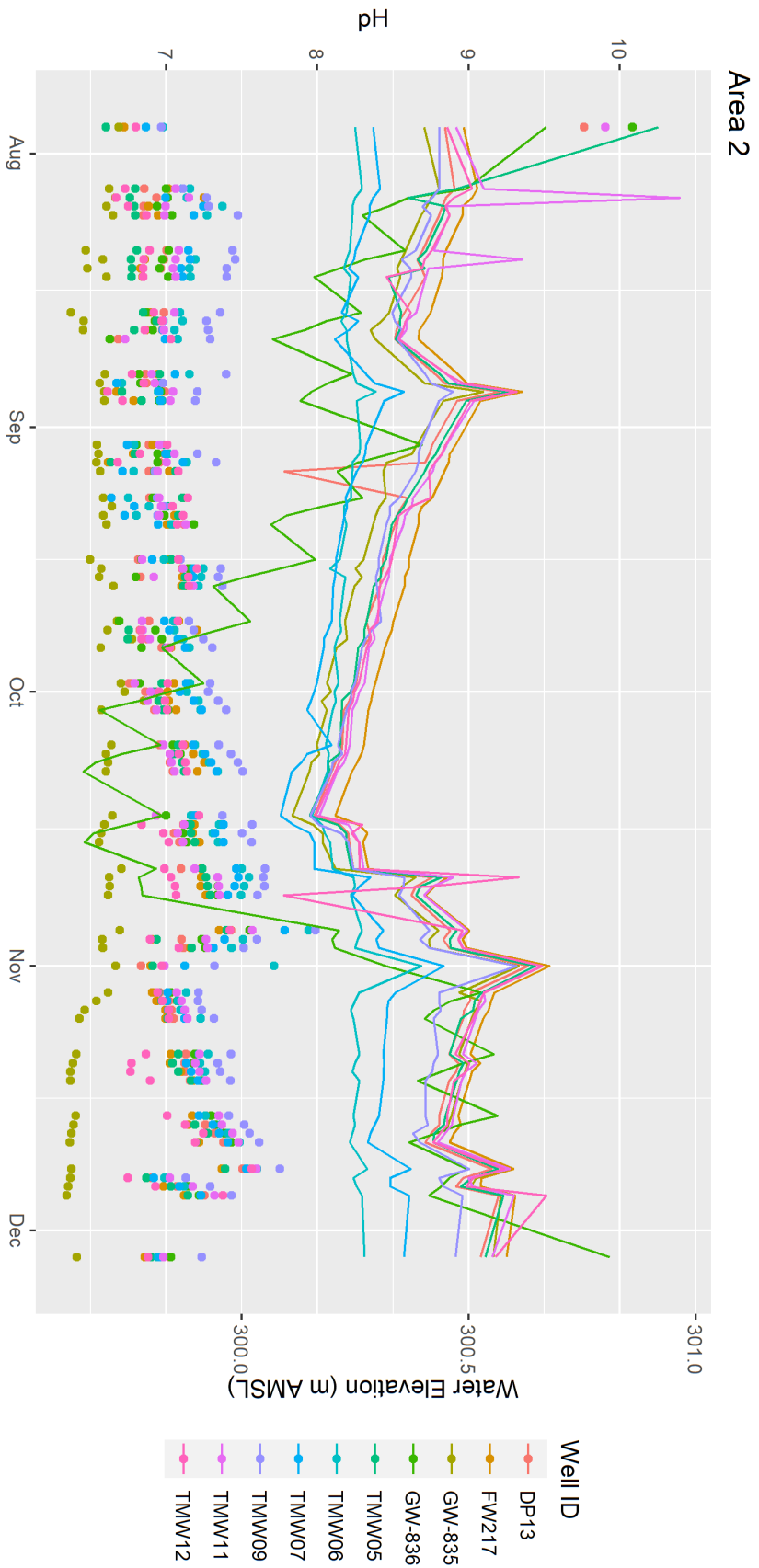


Figure 24: Area 2 – pH (points) and water table elevation in m AMSL (lines)

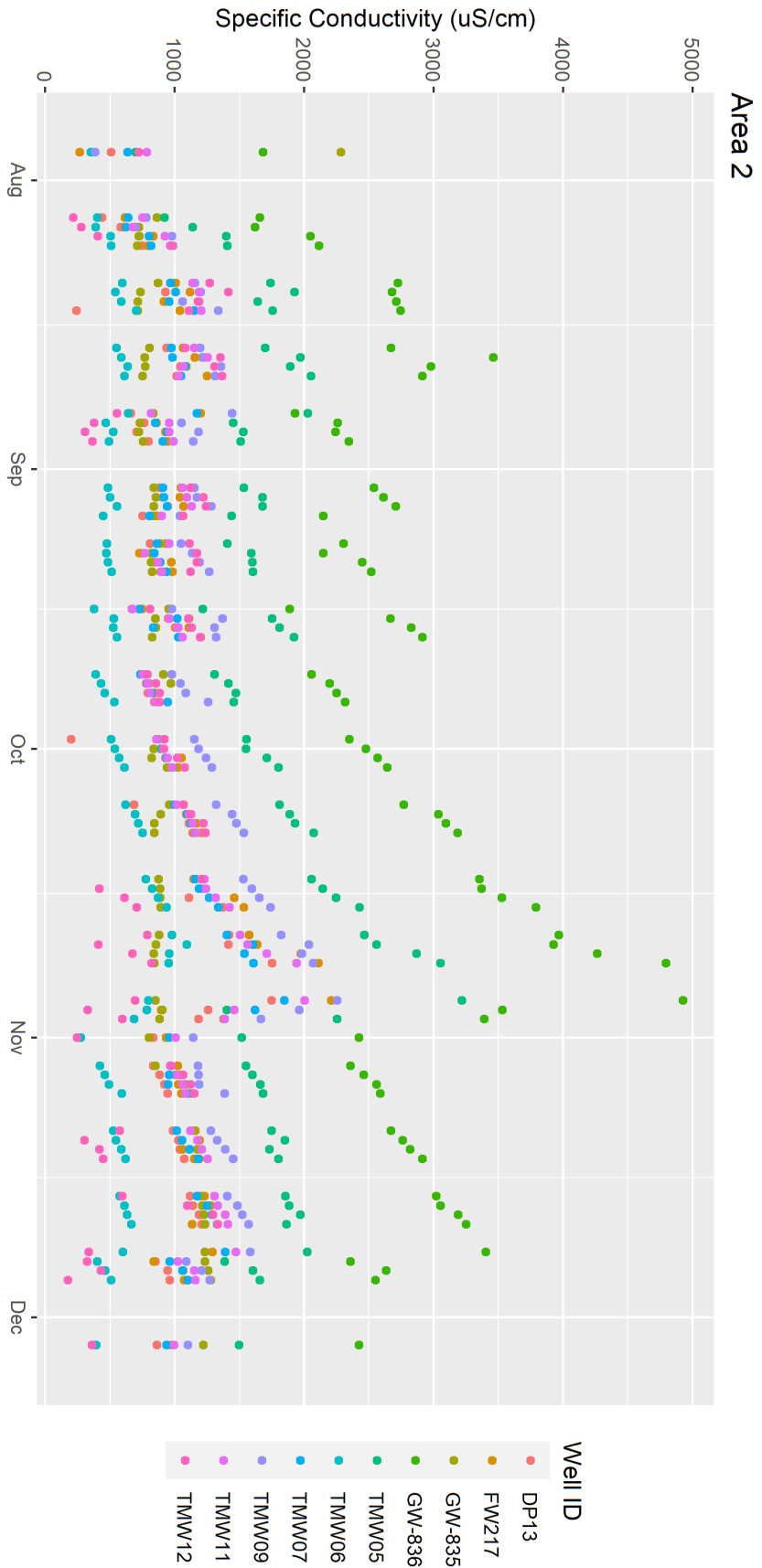


Figure 25: Area 2 – Specific Conductivity in $\mu\text{S}/\text{cm}$ (points) and water table elevation in m AMSL (lines)

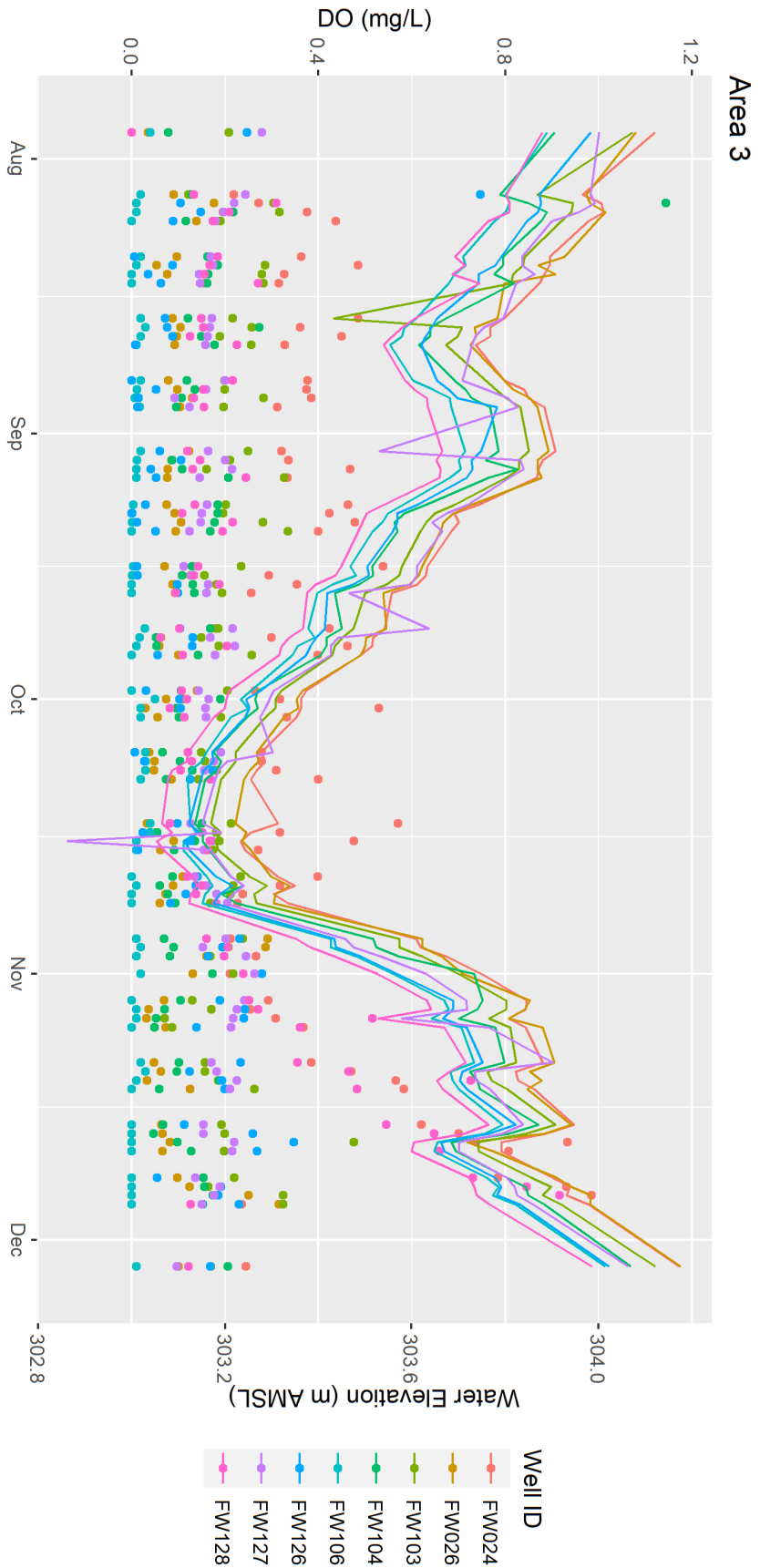


Figure 26: Area 3 – Dissolved oxygen in mg/L (points) and water table elevation in m AMSL (lines)

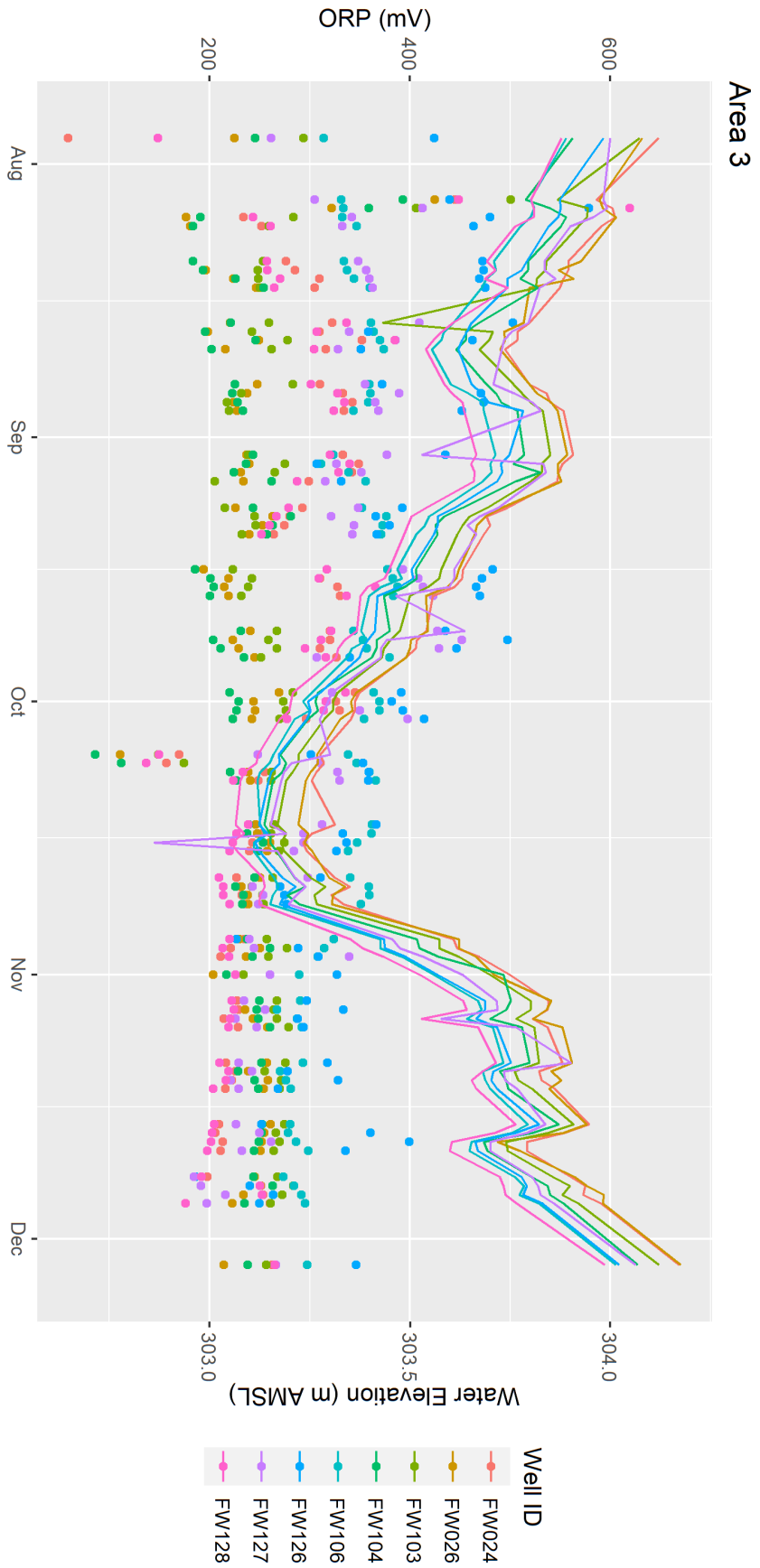


Figure 27: Area 3 – Oxidation-reduction potential in mV (points) and water table elevation in m AMSL (lines)

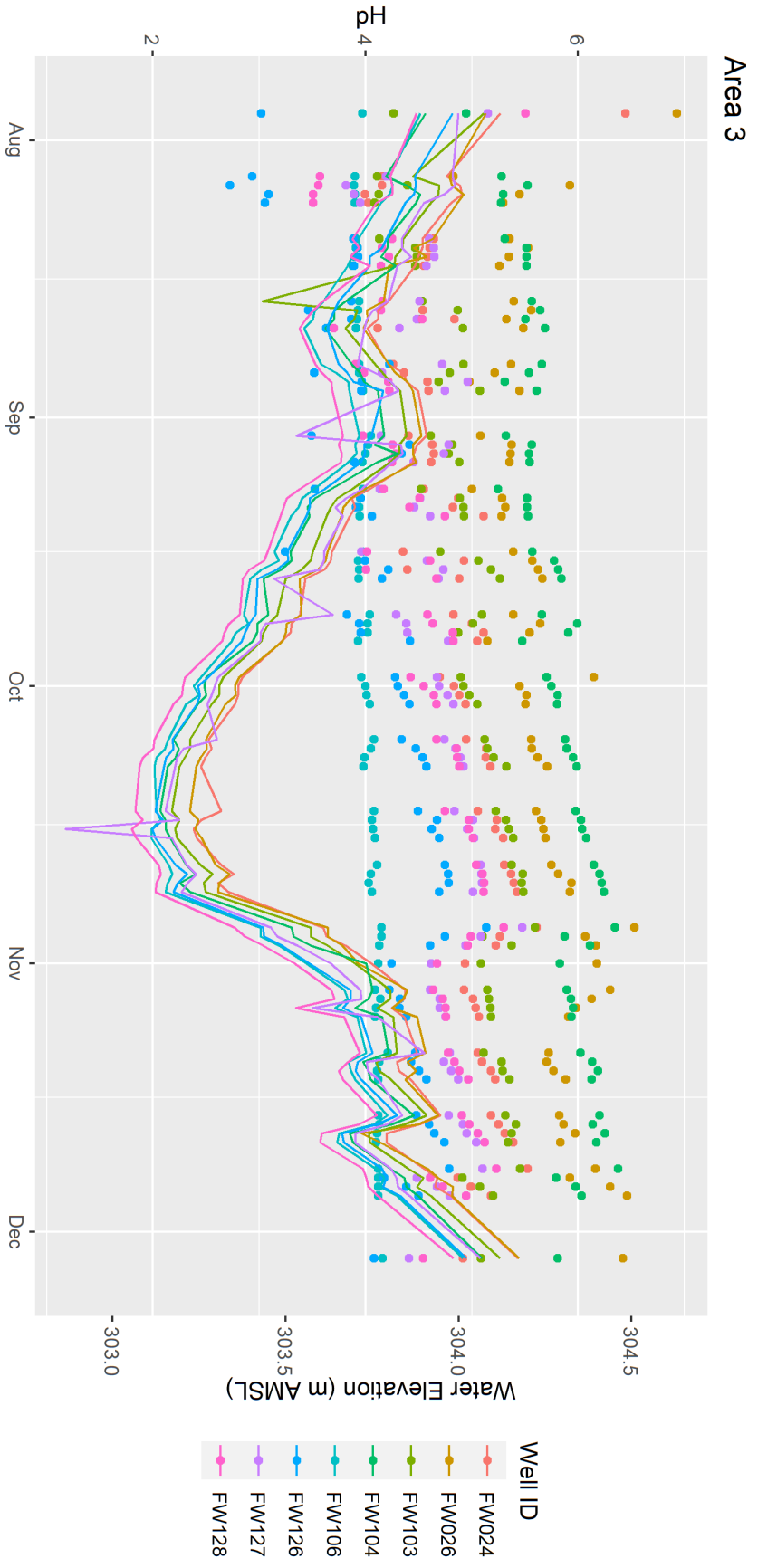


Figure 28: Area 3 – pH (points) and water table elevation in m AMSL (lines)

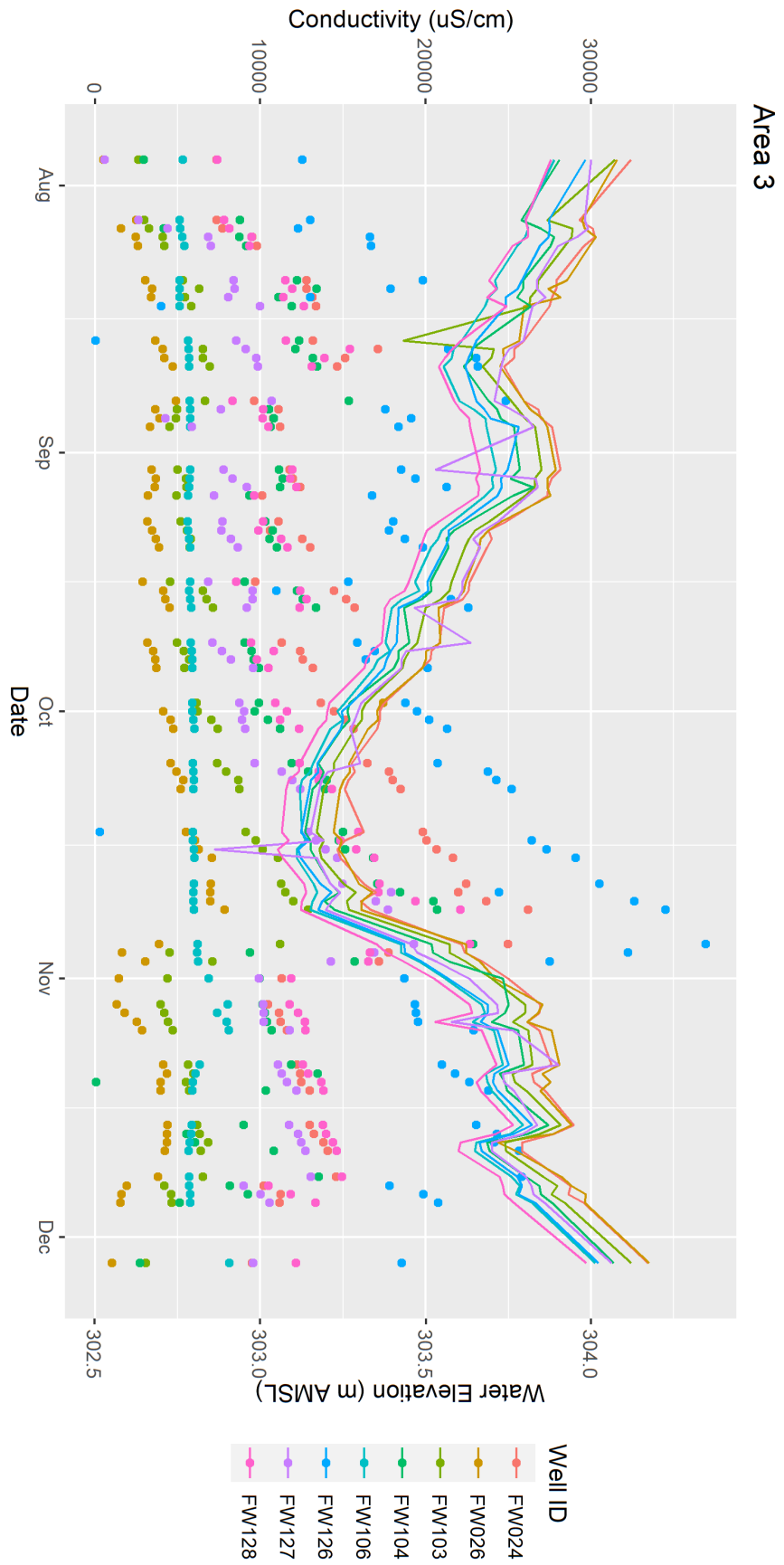


Figure 29: Area 3 – Specific Conductivity in $\mu\text{S}/\text{cm}$ (points) and water table elevation in m AMSL (lines)

Supplemental

[Supplemental.zip](#)

VITA

Emma Dixon graduated with a Bachelor of Science in Civil Engineering from the University of Tennessee, Knoxville in December of 2017. During her undergraduate career, she served as a Resident Assistant for Morrill Hall and as an Engineering Ambassador for the Engineering Professional Practice. She continued to graduate school at the University of Tennessee, Knoxville in January 2018 under the primary advisor Dr. Terry Hazen. She completed the requirements for the Master of Science degree in Environmental Engineering in the summer semester of 2020.